

NUS-4146
REV. 1

ANALYSIS OF FLAMMABLE CONCENTRATIONS
AT THE MIDLAND NUCLEAR PLANT
FROM NATURAL GAS PIPELINE BREAKS

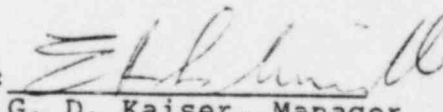
Prepared for

CONSUMERS POWER COMPANY

by

S. J. Nathan H. Firstenberg
P. J. Fulford K. J. Toth
M. Cheok

October 7, 1982

Approved: 

G. D. Kaiser, Manager
Consequence Assessment
Department
Consulting Division

NUS CORPORATION
910 Clopper Road
Gaithersburg, Maryland 20878

TABLE OF CONTENTS

<u>Section and Title</u>	<u>Page No.</u>
1.0 INTRODUCTION	1-1
2.0 NONUNIFORM FLOW FIELD MODELING OF BREAKS ONSITE	2-1
2.1 <u>Introduction</u>	2-1
2.2 <u>Method of Analysis, Three-</u> <u>Dimensional Wind Field Modeling</u>	2-2
2.3 <u>Concentration Fields</u>	2-4
2.4 <u>Summary of Results of the Flow Model</u>	2-7
2.5 <u>Effects of Diffusion</u>	2-8
2.6 <u>Conclusions</u>	2-10
2.7 <u>References for Section 2</u>	2-11
3.0 PROBABILISTIC ASSESSMENT	3-1
3.1 <u>Introduction</u>	3-1
3.2 <u>Method of Analysis</u>	3-1
3.2.1 Frequency of Pipe Rupture	3-3
3.2.2 Determination of Pipe Length of Interest	3-4
3.2.3 Probability of Wind Direction, Stability Category, and Wind Speed, $P_N(n,m,j)$	3-5
3.2.4 Probability of Plume Interception $P_I(k,n,m,i)$	3-6
3.2.5 Probability of Plume Clearance	3-7
3.3 <u>Input Parameters Used</u>	3-11
3.4 <u>Results of Probabilistic Calculations</u>	3-12

TABLE OF CONTENTS (Continued)

<u>Section and Title</u>	<u>Page No.</u>
3.5 <u>Conclusions</u>	3-14
3.6 <u>References for Section 3</u>	3-14

APPENDICES

APPENDIX A	SENSITIVITY OF RESULTS TO GAS EXIT TEMPERATURES	A-1
------------	--	-----

LIST OF TABLES

<u>Table No.</u>	<u>Title</u>	<u>Page No.</u>
2-1	PREDICTED CONCENTRATIONS USING THE IMPACT MODEL	2-12
2-2	PREDICTED MAXIMUM ALLOWABLE RELEASE RATES	2-13
3-1	RESULT SUMMARY - ANNUAL FREQUENCY OF FLAMMABLE GAS CONCENTRATION REACHING SPECIFIC BUILDING AIR INTAKES	3-16
3-2	BUILDING PARAMETERS	3-17
3-3	SENSITIVITY OF FREQUENCY TO BREAK FLOW RATE	3-18
A-1	SPECIFIC GRAVITY EFFECT ON ANNUAL FREQUENCY OF FLAMMABLE GAS CONCENTRATION REACHING SPECIFIC BUILDING AIR INTAKES	A-3
A-2	RESULT SUMMARY OF SPECIFIC GRAVITY EFFECTS ON ANNUAL FREQUENCY OF FLAMMABLE GAS CONCENTRATION REACHING SPECIFIC BUILDING AIR INTAKES	A-4

LIST OF FIGURES

<u>Figure No.</u>	<u>Title</u>	<u>Page No.</u>
2-1	PLANT LAYOUT	2-14
2-2	WIND FIELD ON LEVEL 1	2-15
2-3	WIND FIELD ON LEVEL 2	2-16
2-4	WIND FIELD ON LEVEL 3	2-17
2-5	WIND FIELD ON LEVEL 4	2-18
2-6	HORIZONTAL BOUNDRY LEVEL WINDS	2-19
2-7	CONCENTRATION FLOW -60 LBS/SEC RELEASE RATE	2-20
2-8	CONCENTRATION FLOW -40 LBS/SEC RELEASE RATE	2-21
2-9	CONCENTRATION FLOW -20 LBS/SEC RELEASE RATE	2-22
3-1	DETERMINATION OF PIPE LENGTH OF INTEREST	3-19
3-2	DETERMINATION OF PROBABILITY OF INTERCEPTION	3-20
3-3	PLUME CLEARANCE	3-21
3-4	PIPELINE AND BUILDINGS OF CONCERN	3-22
3-5	PIPELINE AND DISTANCE PERSPECTIVE	3-23

1.0 INTRODUCTION

The purpose of this analysis is to provide a probabilistic assessment of the consequences of a break in the natural gas pipeline which runs to the north of the Midland Plant and from which an inlet section will provide gas for the auxiliary boilers, (See Figure 3-4). This probabilistic analysis is presented in Section 3.0, which contains predictions of the frequency with which flammable mixtures of natural gas and air would occur at the intakes of various structures, (See Table 3-1).

The analysis was carried out based on the assumptions that: both the auxiliary and test boilers will remain in place; the flow rate in the pipeline will be limited to 20 lbs/sec (26,666 scfm) which is approximately 35% greater than the maximum demand required to feed the boilers. The existing main pipeline to the east of the inlet section will be blocked off, (See Figure 3-4). (These criteria were provided by Consumers Power on the basis of preliminary calculations).

The probabilistic analysis was performed using a basic Gaussian dispersion model for a range of stability categories and wind speeds that is representative of the weather conditions occurring at the Midland site. Plume rise was also taken into account using standard formulae developed by Briggs. For each weather condition and each assumed break location, a plume rise calculation was used to see whether the plume would clear the building containing the intake in question and any buildings closer to the break. If the plume was predicted to impact any of these buildings, a non-buoyant dispersion calculation was used.

In the course of the analysis, a question was raised concerning the realism of the basic Gaussian model. In practice, the dispersion of the plume will be influenced by the buildings on the site. This is particularly true for breaks in the inlet sections of the pipeline, between the Evaporator building and the Combination Shop. In order to answer this question, a deterministic calculation of the concentration field caused by various breaks in the inlet section was carried out using a potential flow model that takes into account non-uniformities in the flow fields created by the presence of buildings. This analysis is described in Section 2.0. The modeling showed that if the flow from the break is less than 40 lbs/sec in a 2m/sec wind speed, flammable concentrations will not occur at the Control Room, Auxiliary and Diesel Generator building air intakes and, for flow rates less than 32 lbs/sec, flammable mixtures will not reach the leading edge of the Auxiliary building.

In Section 2.6, there is a discussion of how the realistic analysis can be combined with probabilistic arguments to show that the results of the complete probabilistic analysis of Section 3.0 are reasonable; that is, the realistic analysis is used to demonstrate the robustness of the probabilistic analysis.

The results of the present work, given a limited break flow rate of 20 lbs/sec total, show that the predicted frequency of occurrence of a flammable concentration reaching safety-related building intakes is less than 10^{-7} per year. For example, the frequency at the Control Room, Auxiliary and Diesel Generator building intakes from a break in the pipeline on the perimeter of the site is 6.5×10^{-8} per year, (See Table 3-1).

2.0 NONUNIFORM FLOW FIELD MODELING OF BREAKS ONSITE

2.1 Introduction

The natural gas pipeline that passes north of the site has a tee. From the tee, an inlet section of pipeline comes on-site, (See Figure 3.5). The use of Gaussian plume models to represent transport and dispersion processes for breaks in this immediate area was not appropriate since such models are predicated on the assumption of a uniform wind and dispersion field. An improved and more realistic representation must take into consideration the nonuniformities in the flow fields created by the presence of the buildings. The analysis described below provides a first-order approximation of the solution for the concentration field taking into account the three-dimensional characteristic of the real wind field. The approach used is to obtain a numerical solution for the non-divergent wind field consistent with the arrangement and configuration of the buildings on the plant site. The concentration fields are then simulated by the transport and dispersion of a tracer introduced into the wind field at locations of hypothetical pipeline breaks.

The results of this deterministic potential flow modeling of the complex wind fields show, conservatively, that flammable concentrations will not reach the leading edge of the Auxiliary buildings using a wind speed of 2m/sec and for break flows from the inlet section not in excess of 32 lbs/sec of gas. This rate is 60 percent larger than the 20 lbs/sec maximum required to operate the auxiliary and test boilers. A flow rate of 20 lbs/sec is also used in the probabilistic analysis. For a flow rate less than 40 lbs/sec and a 2.0 m/sec wind speed, flammable concentrations will not reach the Control Room, Auxiliary and Diesel Generator building air intakes.

2.2 Method of Analysis, Three-Dimensional Wind Field Modeling

The modeling of the wind and concentration fields were performed using the IMPACT code.^(2.1) (IMPACT is an acronym for Integrated Model for Plumes and Atmospherics in Complex Terrain). IMPACT uses a finite difference grid model designed to solve air quality problems in complex terrain with spatial and temporal variability in meteorology and chemical transformation of the pollutants. The WEST (Winds Extrapolated from Stability and Terrain) submodel in IMPACT is of primary interest since it is used to determine the three-dimensional, divergence-free wind field for the advection calculations. The numerical algorithm in WEST, as described in Reference 2-1, consists of solving for the face-centered velocities in the computational grid using perturbation potentials and directionally-dependent transmission coefficients. Comparisons of the WEST submodel and the MATHEW code^{2.2} are also given in Reference 2.1.

The application of the IMPACT code to simulate the wind fields at the Midland Plant makes use of the ability of the WEST submodel to treat velocity fields in complex terrain. The buildings are represented by obstacle cells in the grid, that is, cells on whose boundary the velocity components are zero. Resolution of the building arrangement and configuration on the plant site was achieved by a 40 cell x 56 cell x 10 cell cartesian grid with each cell being 20ft x 20ft x 20ft. Figure 2-1 shows the main buildings and structures represented in the model. The solution was initiated by constraining the wind vector at one location in the first row and first level and allowing WEST to calculate the nondivergent, three-dimensional wind field consistent with the boundary conditions. The resultant cell-centered winds from WEST are shown in Figures 2-2 to 2-5 for the first four levels in the grid.

The open cells in these figures correspond to the obstacle cells of buildings and structures depicted in Figure 2-1.

The lines shown in Figure 2-2 through 2-5 are representations of the cell-centered, horizontal wind vectors predicted by the IMPACT model for the first four levels in the numerical simulation. The length of these wind vectors gives the calculated wind speed when referenced to the length of VMAX shown in the lower left hand corner of each figure. These figures provide a pictorial representation of how the horizontal components of the three-dimensional wind are influenced by the presence and configuration of flow obstacles at the Midland Nuclear Power Plant. The upper row of cells in each figure can be observed to have parallel cell-centered wind vectors which depict the conditions of the undisturbed wind field. Progressing down through the rows, one can see the wind vectors begin to turn upwind of the flow obstacles. Where the pressure gradients favor a horizontal deflection of the winds, for example, near the edges of the structures, the horizontal windspeed can be seen to increase. This arises from the greater flow of air through fewer cells. The opposite effect on the windspeed can be observed at the corner regions in the lee of the obstacle where the winds also preferentially relax in the horizontal direction. The alley between the Evaporator and Combination Shop buildings is a region of accelerated, horizontal winds caused by the tendency for greater horizontal relaxation of the air flow around the corners of these buildings adjacent to the alley.

As one moves away from the corners on the leading edge of the obstacles, the characteristics of the horizontal wind field noticeably change. The horizontal component of the cell-centered wind vectors can be seen to decrease near the flow

obstacle. These are regions in which the air is preferentially forced to flow up and over the structure rather than around the structure. The winds experience an upward acceleration on the windward-side and a downward acceleration on the leeward-side of the flow obstacle. The further the distance from the edges of the building, the stronger will be the tendency for the air to move over the building. Clearly, as one moves away from the edges, one finds a mixed situation with some of the air moving vertically and some moving horizontally. Figure 2-6 shows the horizontal wind field in those cells adjacent to obstacle cells in the problem; that is, the horizontal components of the cell-centered winds in those cells above solid, horizontal boundaries in the simulation. Although the obstacle cells are not shown in this representation, the general pattern of the flow field is clearly visible in this composite figure.

The complexity of the three-dimensional wind field caused by the on-site buildings and structures is evident from these figures. A neutrally buoyant material introduced in such a flow field will be diluted, in part, merely by the advective motions and mixing of the air. Since the IMPACT code only deals with nondivergent flows, the enhanced mixing attributable to the turbulent wake of the structure cannot be represented. In this context, the concentrations predicted by this methodology will be higher than those expected under actual conditions. An estimate of the effect of the turbulent wake is made below using enhanced dispersion parameters developed from wind tunnel studies.

2.3 Concentration Fields

Once the direction of the undisturbed wind vector is established, the potential wind field calculated by WEST will

scale directly to the undisturbed wind speed; that is, the perturbed wind vectors retain the same direction but their length (wind speed) is directly proportional to the undisturbed wind vectors everywhere in the field. The concentration field, however, will depend on the location of the tracer source in the field. A tracer is a material distinguishable from air but assumed to have properties that do not cause perturbations to the wind field. Three natural gas pipeline accident scenarios were investigated in this study. Two involved assumed guillotine breaks in the high pressure lines -one just upstream of the pressure reducing station near the Evaporator building and the other at the tee-section where the two branch lines join. The third accident scenario involved a guillotine break in the low pressure line between the Evaporator and Combination buildings. These locations are shown on Figure 2-1. To calculate the concentration field, it was conservatively assumed that the natural gas behaved as a neutrally buoyant tracer and that the wind field was non-diffusive. Thus, the natural gas concentrations were determined solely by advection of the tracer gas through the wind field.

Figure 2-7 illustrates the plume concentrations predicted by this model in vertical planes between the reactor containment buildings. The concentration isopleths (lines of constant concentration) correspond to 1.0 v/o (volume percent) and 5.0 v/o natural gas in air mixtures for a high pressure pipeline break at the pressure reducing station with an arbitrary 60 lbs/sec flow rate and an undisturbed wind speed of 2.0 meters/second. The 0.5 percentile meteorology for winds from the North correspond to 2.0 m/sec and D-stability. Winds from adjacent sectors have higher wind speeds at the corresponding 0.5 percentile meteorology collected from the

on-site tower and lead to lower predicted concentrations. The influence of the wind field on the concentration field is very evident from Figure 2-7. The upper sketch shows the contour of the lower flammability limit (5.0 v/o) just reaching the leading edge of the Auxiliary building. On the other hand, the adjacent vertical cells show a tongue of flammable gases carrying over the Auxiliary building, between the Reactor Containment buildings, and terminating on the upwind side of the Turbine building. Thus, the model predicts that flammable concentrations of natural gas can occur in the vicinity of the Control Room and Auxiliary building ventilation air intakes for this postulated 60 lbs/sec accident. The cross-sections shown in Figure 2-7 are 20 feet apart, corresponding to the minimum resolution of the computational grid, and illustrate the steepness of the horizontal concentration gradients obtained with this modeling approach. In part, this arises from the assumption of a nondiffusive wind field used in the analysis. Diffusion will tend to smooth out the horizontal concentration gradients and lower the maximum concentration levels predicted with the model. As will be seen in Section 2.5, the dilution of the tracer will still be dominated by advective mixing even when enhanced dispersion in the wake of the Evaporator and Combination Shop buildings is incorporated in the analysis. It is pertinent to observe that the predicted concentration levels will depend on the flow rates. From Figure 2-8, it can be seen that flammable mixtures are not predicted in the vicinity of the Control Room and Auxiliary building air intakes when the break flow rate is at 40 lbs/sec or less. Similarly, Figure 2-9 shows that concentration levels at or above the Auxiliary building remain below the lower flammability limit for a 20 lbs/sec pipeline break flow rate.

2.4 Summary of Results of the Flow Model

The results of the maximum concentrations predicted at (1) the leading edge of the Auxiliary building, (2) the top of Auxiliary building, and (3) the general vicinity of the Control Room and Auxiliary building air intakes are presented in Table 2-1 for different accident scenarios. Since dispersion of the natural gas was considered to occur by advective mixing only, both high pressure accident scenarios gave essentially the same concentrations and so only a single result is shown. On the basis of these results, it is possible to determine a natural gas leak rate from a pipeline break that would just cause a flammable mixture at the above three locations. These maximum allowable leak rates are shown in Table 2-2 and are determined from the predictions of a break in the high pressure side of the pipeline.

The results for the low pressure pipeline break were modeled with the release occurring in either the first or second level of the grid. This was done to determine the sensitivity of these predictions to the height of release. The concentrations summarized in Table 2-1 for the two low pressure breaks require some further explanation insofar as the model seems to predict an anomalous behavior in the concentration fields. This is a reflection of the three-dimensional character of the flow field implicit in this approach to the analysis, which, in turn, causes the tracer to behave differently when released at different locations in the flow field. For the low level release, the tracer plume experiences a pronounced easterly deflection when it encounters the flow obstruction represented by the Auxiliary and east Reactor Containment buildings. An examination of the model results shows that most of the tracer flows around the

east Reactor Containment building, being deflected upward by the Turbine building and causing a maximum concentration of 2.6 v/o to occur on the leeward side of the containment structure. As noted in Table 2-1, this location of maximum concentration level was taken to be associated with the vicinity of the Control Room and Auxiliary building air intakes and the top surface of the Auxiliary building, although for the latter it might be more appropriate to consider it atop the Turbine building. The portion of the tracer plume transported up and over the Auxiliary building leads to a maximum concentration of 0.8 v/o on the top surface, thereby indicating the extent to which the tracer plume is deflected toward the East. An entirely different behavior is predicted for the elevated low pressure break, since most of the tracer plume moves up and over the Auxiliary building between the two Reactor Containment structures. Some tracer is deflected eastwardly around the Reactor Containment building, but the concentration levels show this portion of the plume to transport considerably less tracer material.

2.5 Effects of Diffusion

The enhanced turbulent diffusion in the wake of sharp-edged buildings was investigated for the high pressure pipeline breaks. To simulate this effect, a diffusive region was assumed to exist between the Evaporator and the Combination Shop buildings and the front of the Auxiliary building. The height of the diffusive region was conservatively chosen to be equal to the respective heights of the Evaporator and Combination Shop buildings in the downwind zone behind each building. This representation created a volume of diffusive air through which the plume was transported before impacting the modeled area of greatest concern. The remainder of the

wind field was still considered nondiffusive as in the earlier analyses. The eddy diffusivities were estimated from the equations

$$K_y = u_x \sigma_y \frac{d\sigma_y}{dx} = K_x$$

and

$$K_z = u_x \sigma_z \frac{d\sigma_z}{dx} = K_x$$

where σ_y and σ_z are the Huber-Snyder dispersion parameters^(2,3) in the wake of a sharp-edged building and the coordinate system oriented with the x-direction collinear with the wind vector and the positive z-direction measured upward from the ground plane. Using the dimensions of the buildings, one obtains $K_x = K_y = 0.055$ meter²/second and $K_z = 0.11$ meter²/second in the wake of the Combination Shop building and $K_x = K_y = 0.038$ meter²/second and $K_z = 0.11$ meter²/second in the wake of the Evaporator building. The transition region was assigned the arithmetic mean of the zones behind the Evaporator and Combination Shop buildings.

Although the concentration field was changed by the large eddy diffusivities assigned to the region between the Evaporator and Combination Shop buildings, the effect on the maximum concentrations at the same locations in the earlier analyses were not very dramatic. The maximum concentration predicted at the leading edge of the Auxiliary building was lowered by about 22% and in the vicinity of the Control Room and Auxiliary building intakes by about 17% when compared to the non-diffusive model. Thus, turbulent diffusion has a second-order effect on the concentration field as compared to the influence of the wind field. The effect of the diffusion is thus

indicated to be conservative, i.e., the results discussed in Section 2.4 and shown in Table 2-1 are concentrations at the intakes that are actually higher than what one would expect to calculate using a full 3D model that explicitly included diffusion effects.

2.6 Conclusion

Using the potential flow model described in this section, it has been shown that if the flow from the break does not exceed 40 lbs/sec, flammable concentrations will not occur at the Control Room and Auxiliary building air intake in a wind speed of 2.0 m/sec. Since concentrations in the modified flow model are inversely proportional to wind speed, flammable concentrations will not occur at the Control Room and Auxiliary building air intakes for a flow rate less than 40 lbs/sec and a 2.0 m/sec wind speed or a flow rate of 20 lbs/sec and a wind speed exceeding 1 m/sec.

The probability of a break in the inlet pipe, which is about 400' in length, is:

$$400 \times 3.31 \times 10^{-8} = 1.3 \times 10^{-5} \text{ per year. (See Section 3.0)}$$

The probability that the wind will blow from the North or the two adjacent sectors, with a wind speed of less than 1 m/sec, is 1.1×10^{-3} . Hence, the predicted frequency with which breaks in the inlet pipe would cause flammable concentrations to occur at the Control Room and Auxiliary building air intake is about 1.4×10^{-8} per year. This estimate is close to that obtained from the full probabilistic analysis of Section 3.0, see Table 3-1, and serves to add credibility to the results.

2.7 References for Section 2

- 2.1 Fabrick, A., R. Sklarew and J. Wilson, "Point Source Modeling: State-of-the-Art Assessment of Computer Simulation of Localized Air Pollutant Emissions," Form and Substance, Inc., September 1977. IMPACT-ERA-82A1B
- 2.2 Sherman, C.A., "A Mass-Consistent Model for Wind Fields Over Complex Terrain," UCRL-76171, 1976.
- 2.3 Bowers, J.F., J.R. Bjorklund and C.S. Cheney, "Industrial Source Complex (ISC) Dispersion Model User's Guide: Volume I," EPA 450/4-79-030, December 1979.

TABLE 2-1

PREDICTED CONCENTRATIONS USING THE IMPACT MODEL

Release Characteristics*	Resultant Concentration (v/o)		
	Leading Edge	Top Surface	Control Room
	Aux Bldg	Aux Bldg	Intakes
Low Pressure Line Break (Ground Level) 15.4 lbs/sec	1.4	2.6**	2.6**
Low Pressure Line Break (Elevated Level) 15.4 lbs/sec	3.5	2.4	2.0
High Pressure Line Break (Ground Level) 60 lbs/sec	9.5	8.6	7.4

*See Figure 2-1 for break locations.

**Concentration occurs in the leeward side of the east Reactor Containment building and is taken to be the same for the top surface of the Auxiliary building and the Control Room intakes (see discussion in Section 2.4).

TABLE 2-2

PREDICTED MAXIMUM ALLOWABLE RELEASE RATES

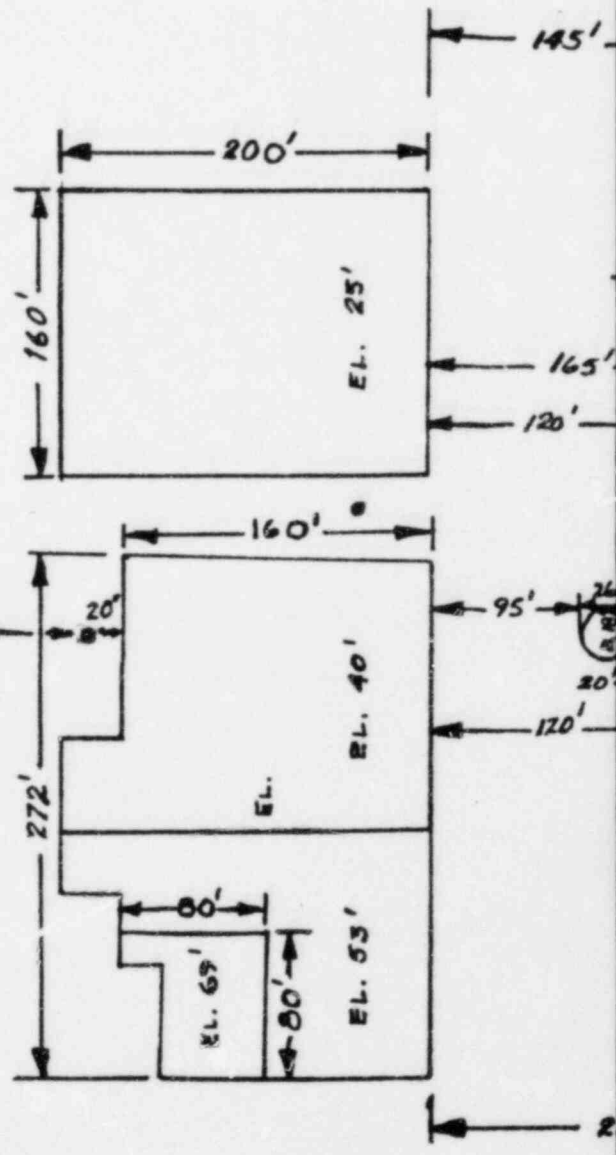
(To assure concentrations less than 5 v/o)

<u>Location</u> <u>Auxiliary Building</u>	<u>High Pressure Line</u> <u>Max. Break Flow Rate</u>
Leading Edge	32 lbs/sec
Top Surface	35 lbs/sec
Control Room Intakes	40 lbs/sec

CLOSED SECTION OF PIPELINE

INLET SECTION OF PIPELINE

PERIMETER SECTION OF PIPELINE



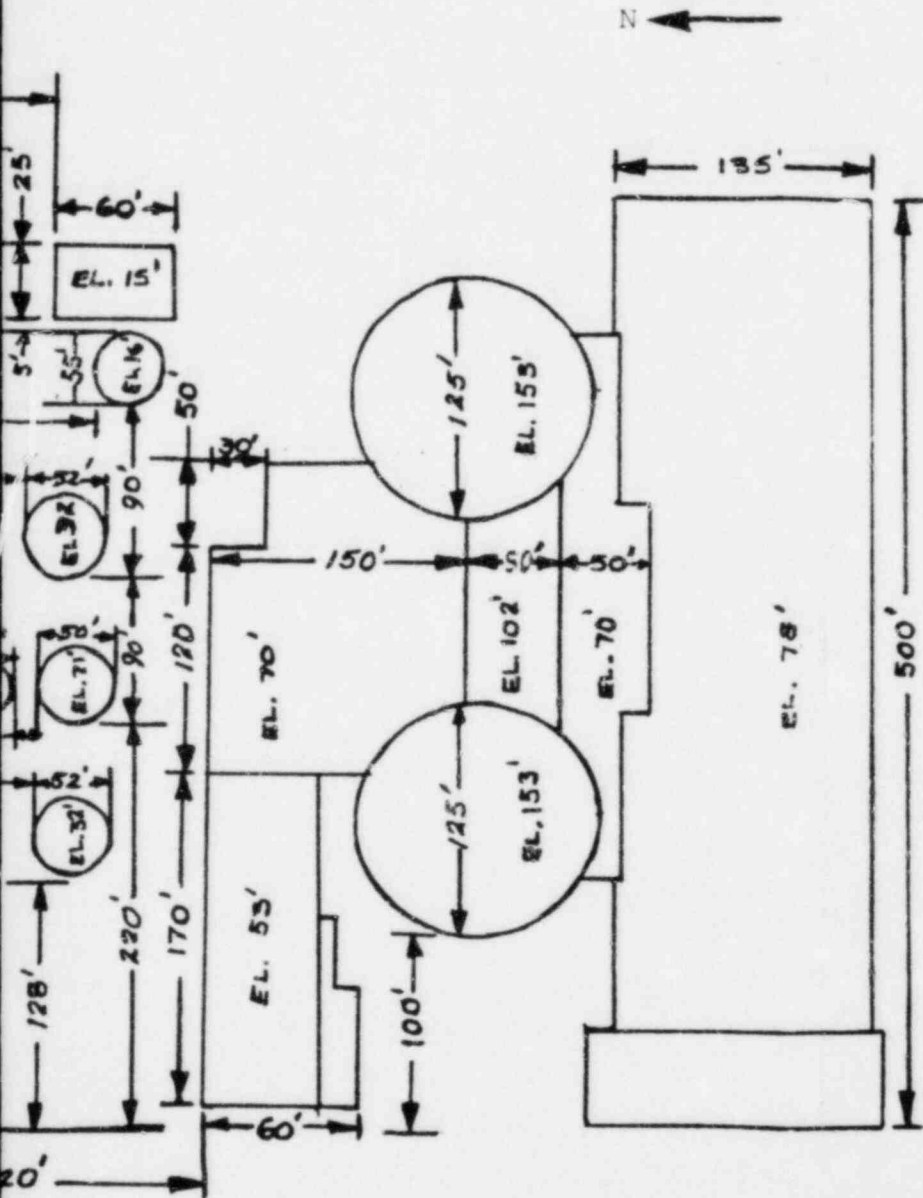


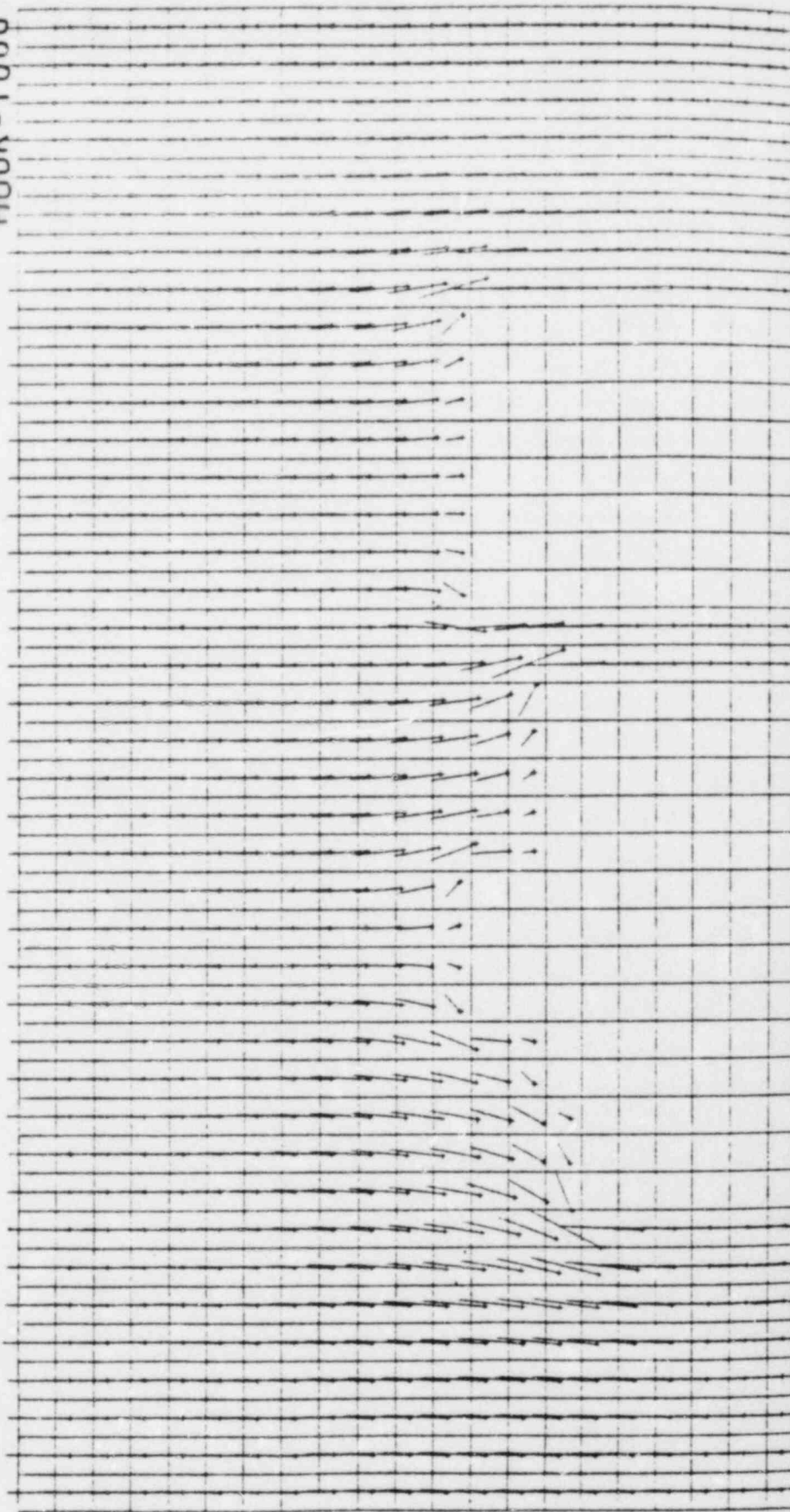
FIGURE 2-1

MIDLAND NUCLEAR POWER STATION
 BUILDING'S ARRANGEMENT FOR INPUT
 IMPACT COMPUTER CODE ANALYSES

● LOCATION OF BREAKS

HOUR = 1000

VMAX-2.00 M/S



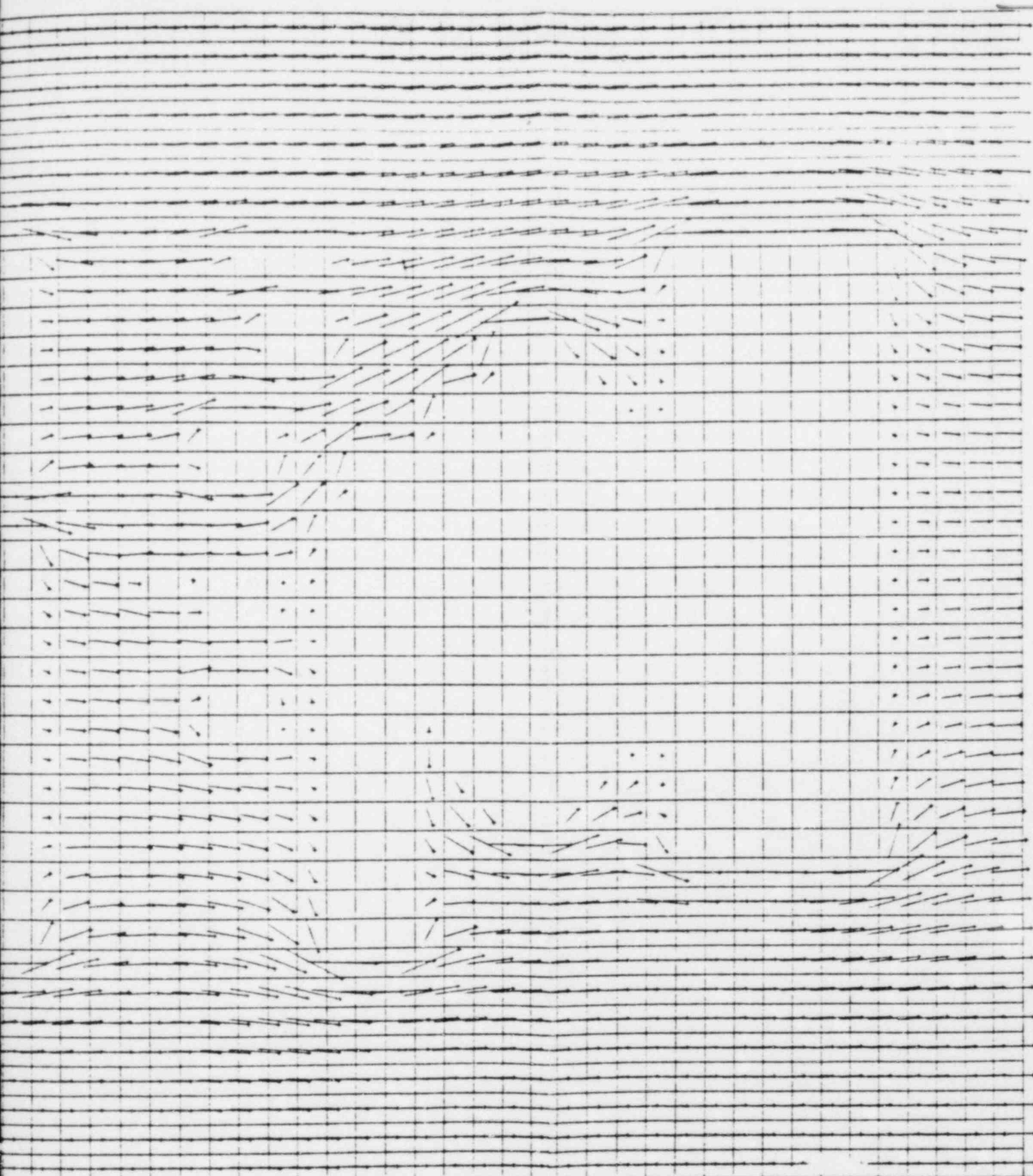
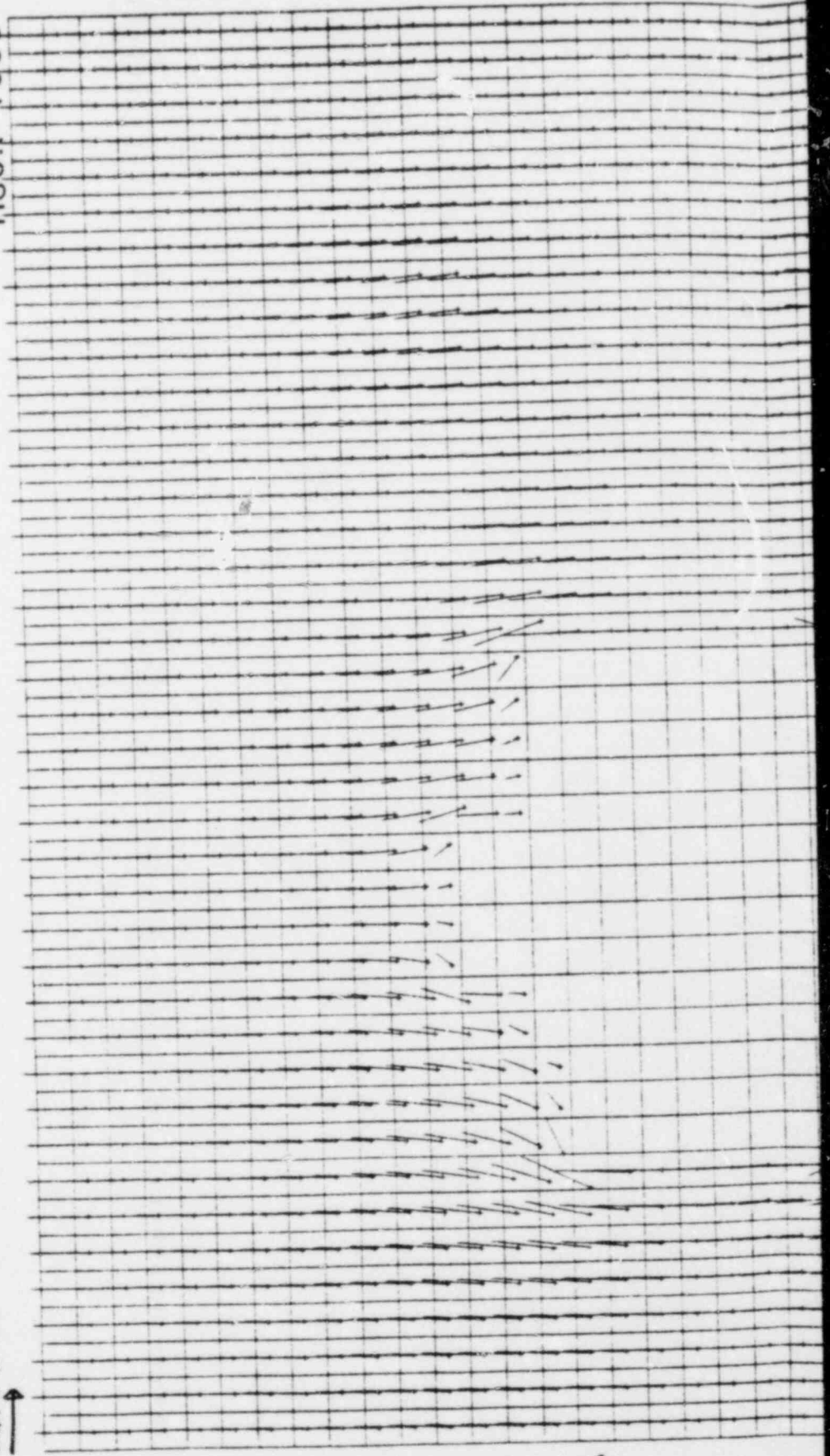


FIGURE 2-2
WIND FIELD ON LEVEL 1 (0'-20')
40x56 GRID 2 M/S INPUT

HOUR = 1000

V_{MAX} = 2.00 M/S



→ Z

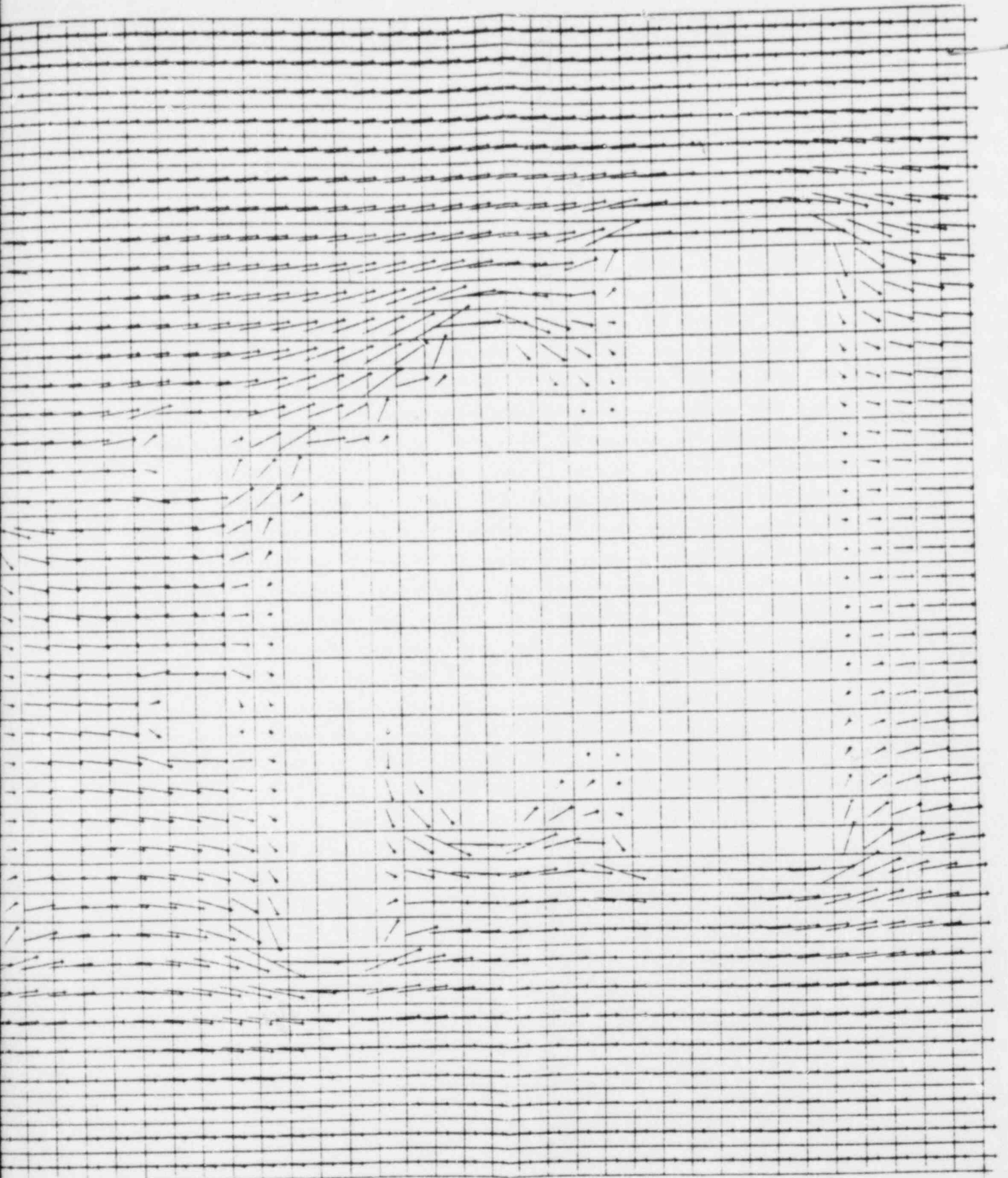
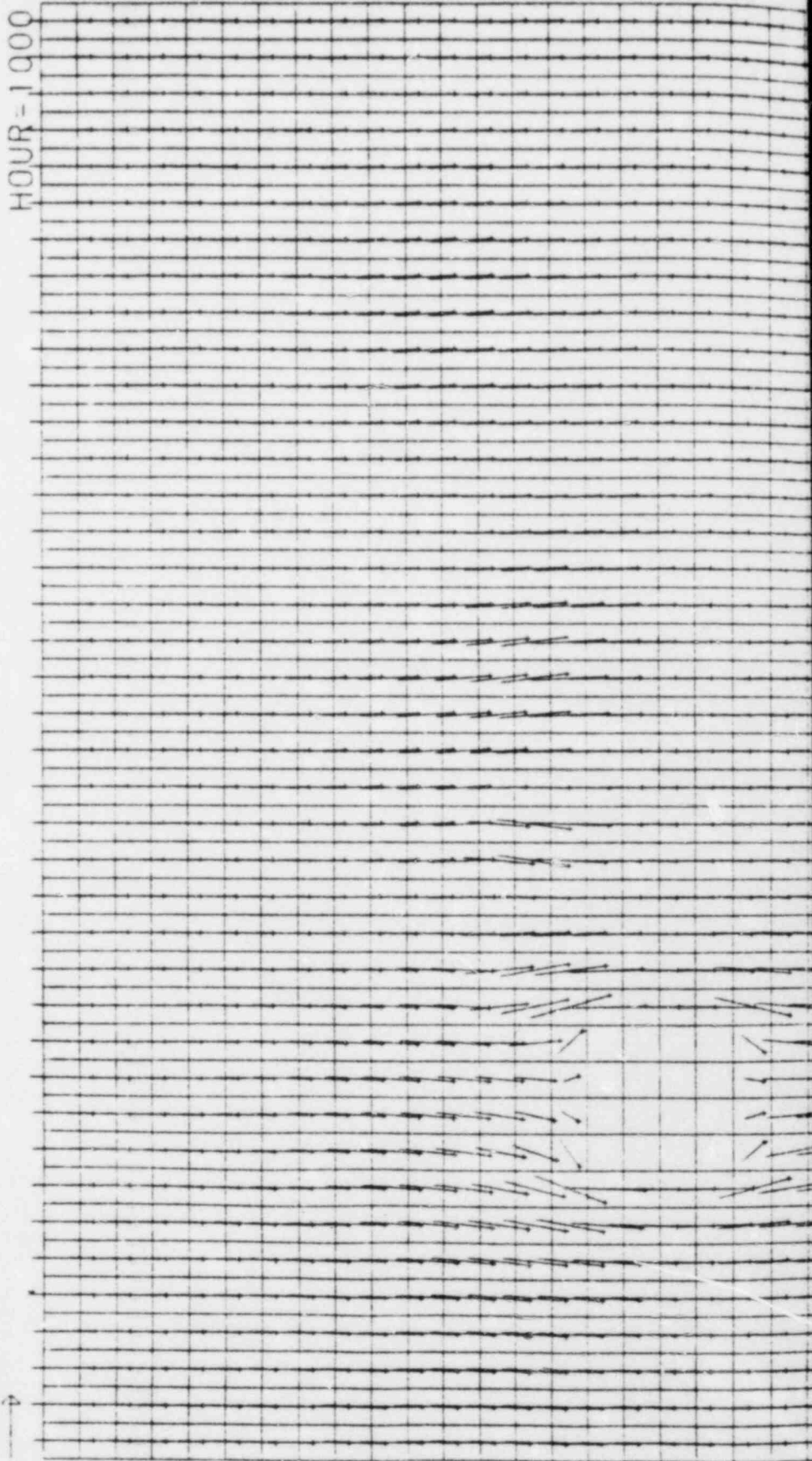


FIGURE 2-3
WIND FIELD ON LEVEL 2 (20'-40')
40x56 GRID 2 M/S INPUT

HOUR = 1000

VMAX = 2.00 M/S



↖ N

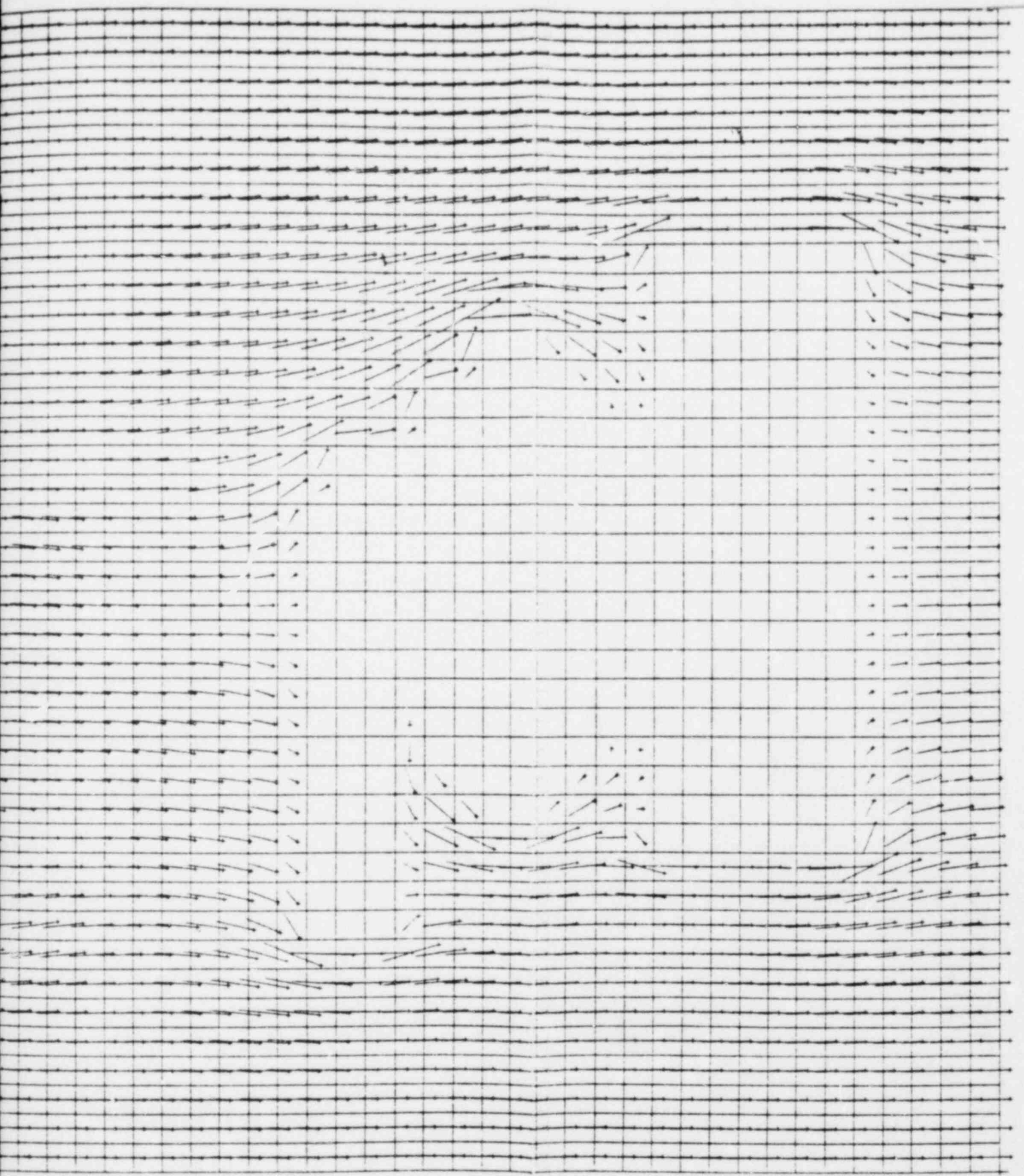
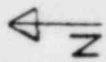
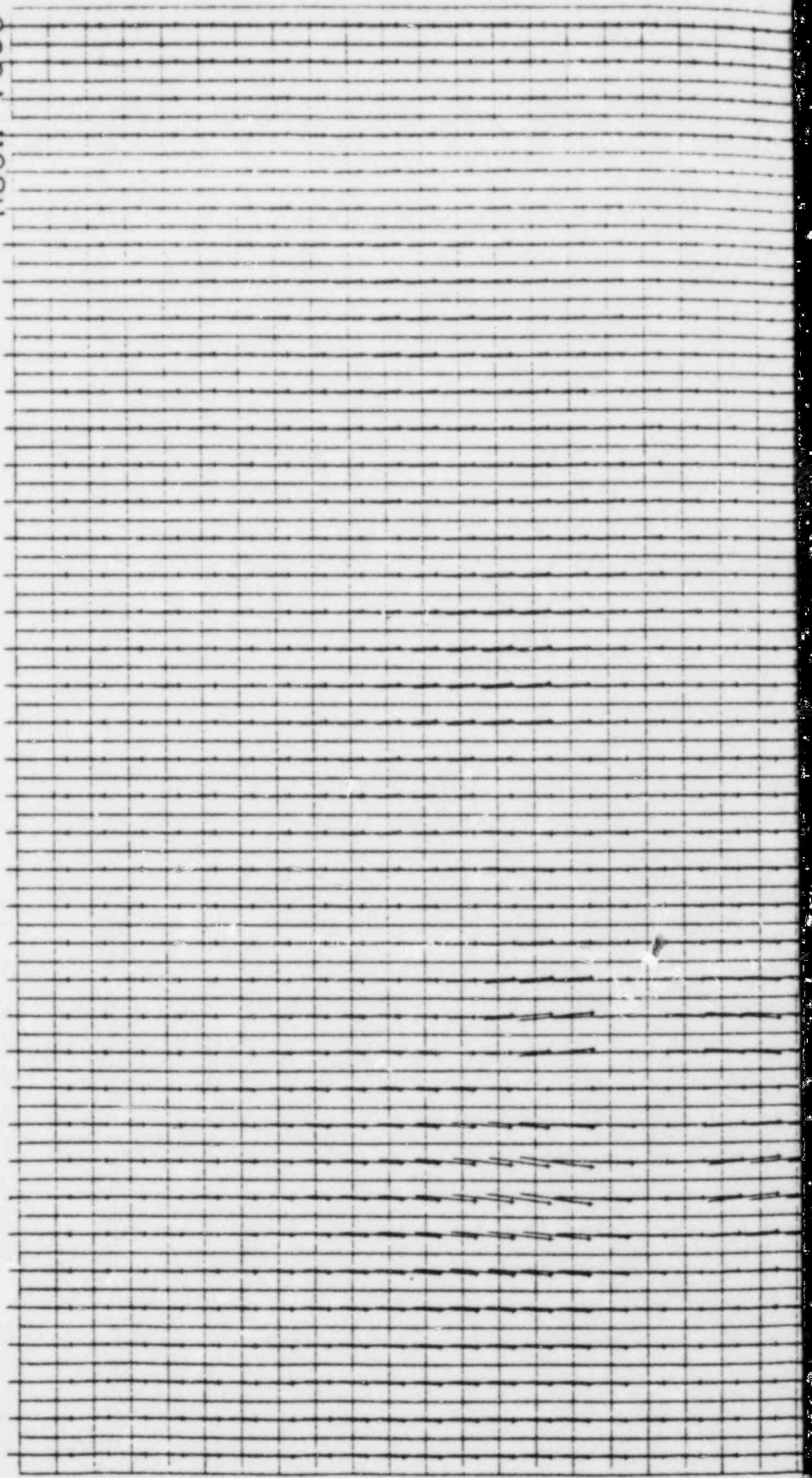


FIGURE 2-4
WIND FIELD ON LEVEL 3 (40'-60')
40x56 GRID 2 M/S INPUT

HOUR = 1 000

VMAX = 2.00 M/S



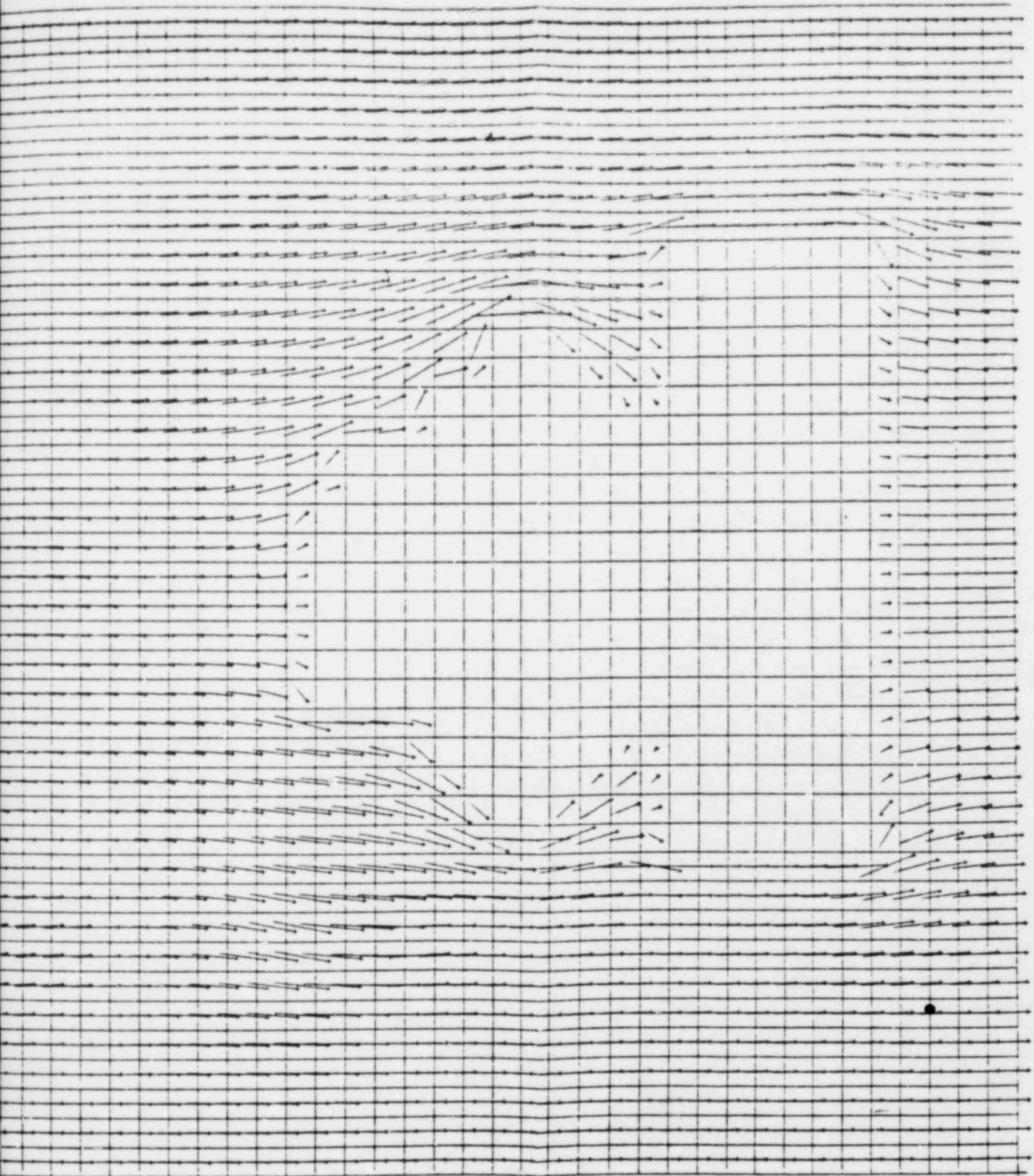
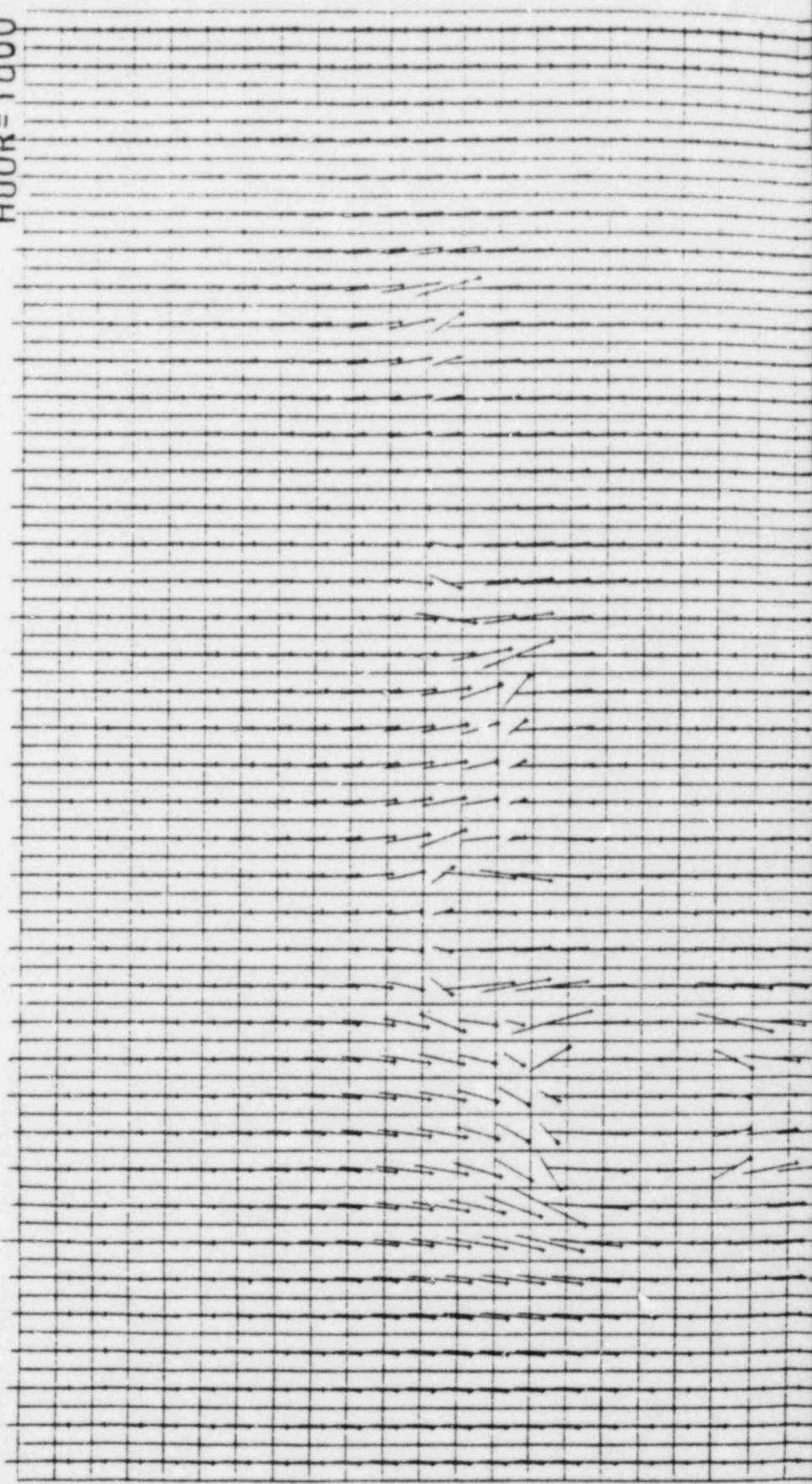


FIGURE 2-5
WIND FIELD ON LEVEL 4 (60'-80')
40x56 GRID 2 M/S INPUT

HOUR = 1000

VMAX = 2.00 M/S



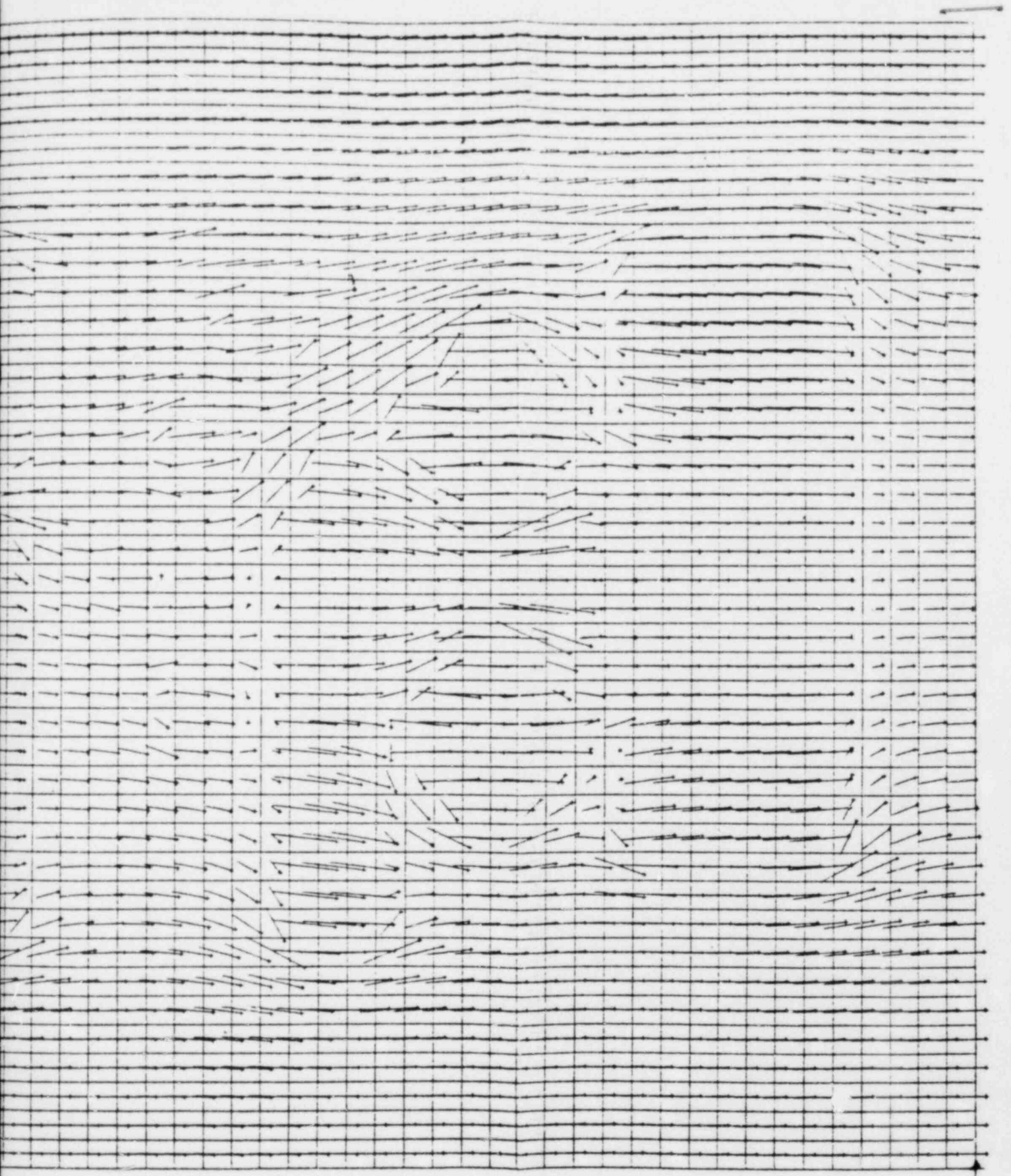


FIGURE 2-6
HORIZONTAL BOUNDARY LEVEL WINDS

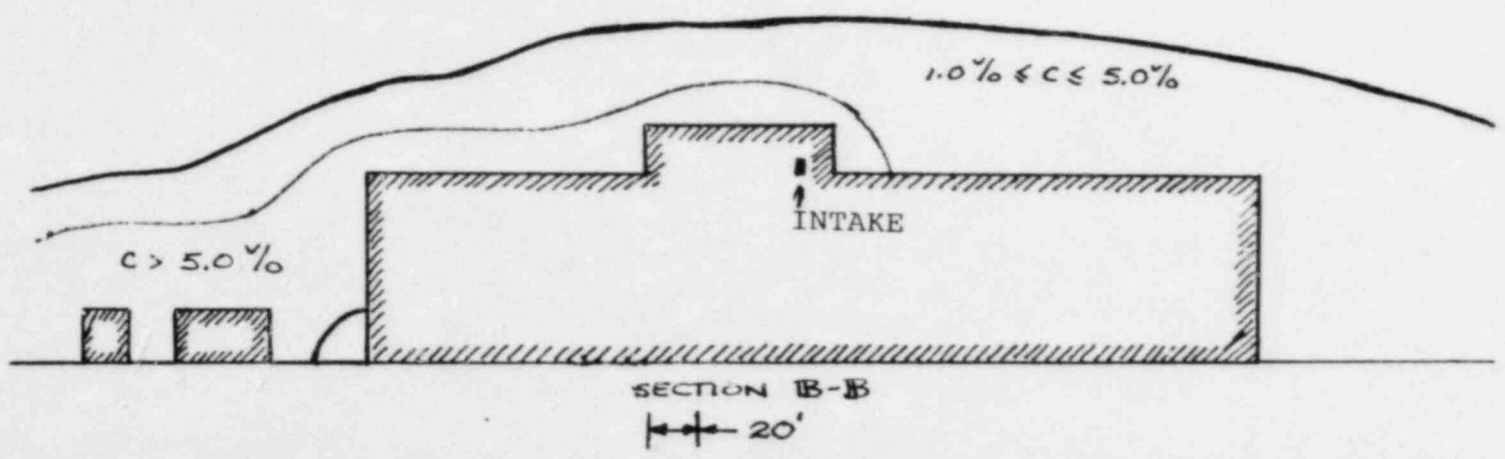
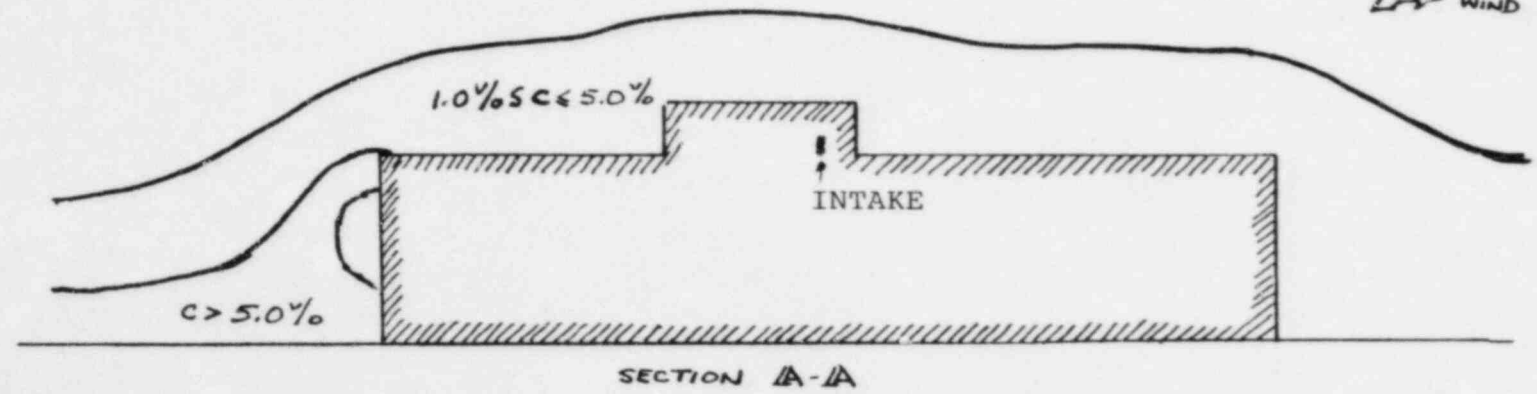
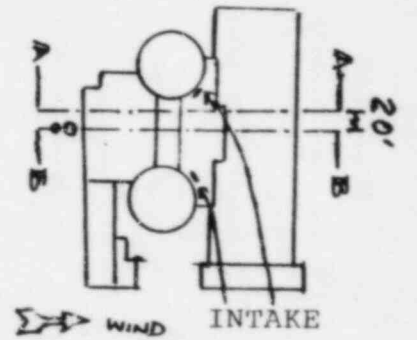
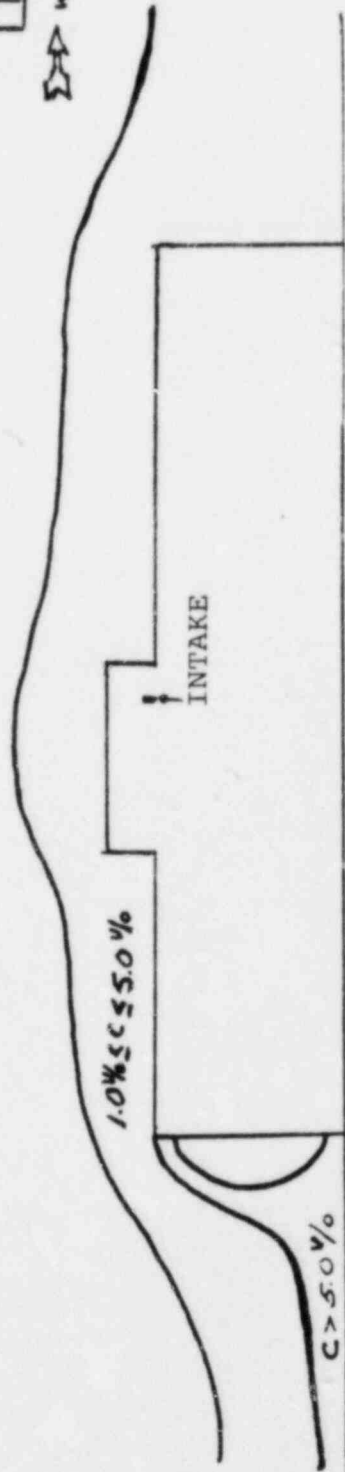
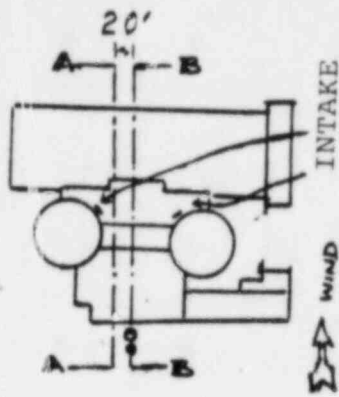
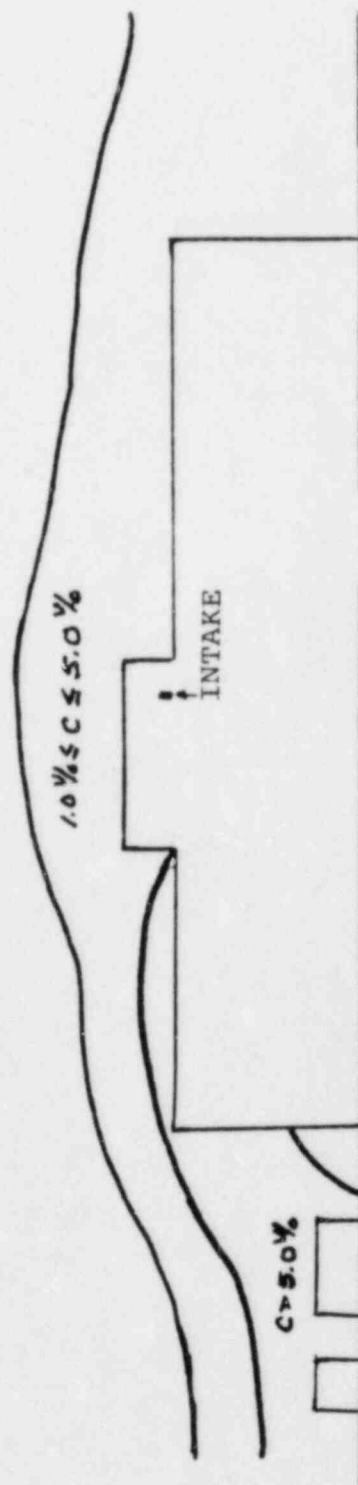


FIGURE 2-7
CONCENTRATION FLOW -60 LBS/SEC
RELEASE RATE



SECTION A-A

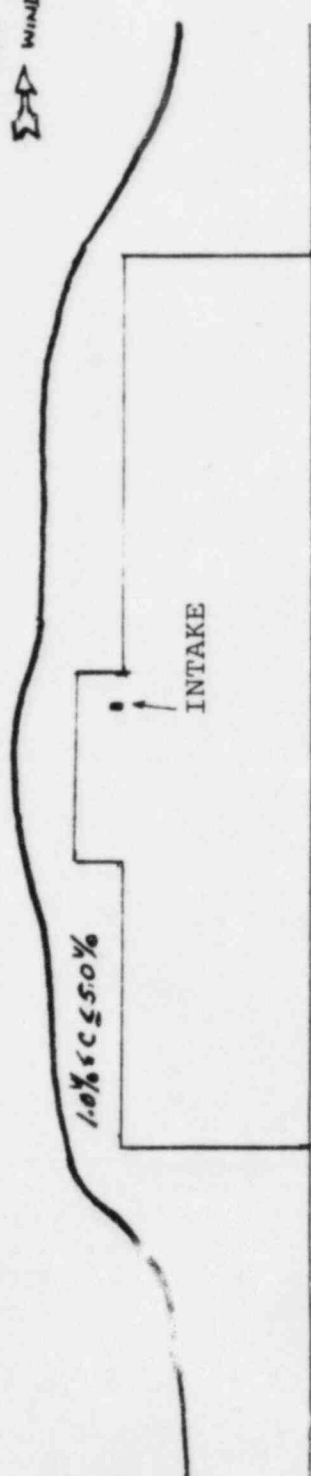
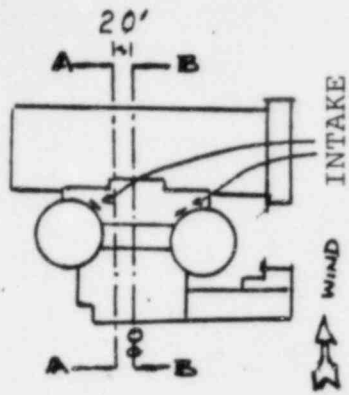
WIND
2.0 METERS/SEC



SECTION B-B

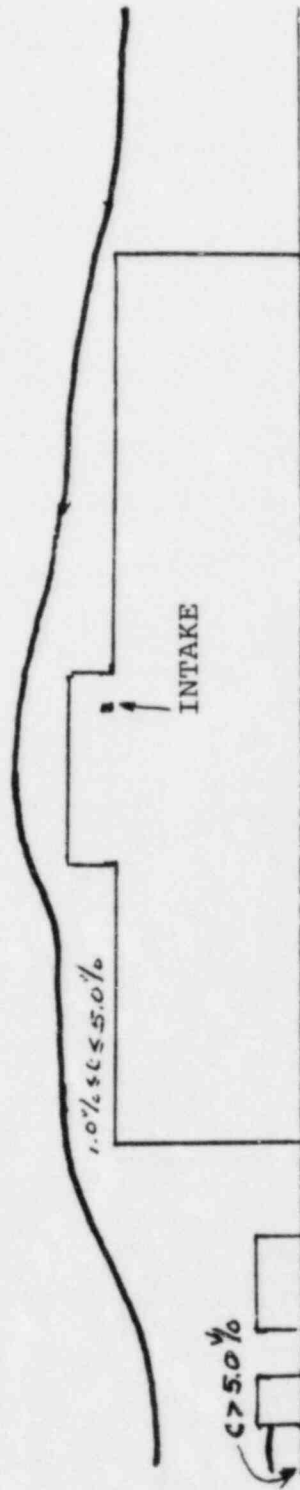
← 20'

FIGURE 2-8
CONCENTRATION FLOW -40 LBS/SEC
RELEASE RATE



SECTION A-A

WIND
2.0 METERS/SEC.



SECTION B-B

← 20'

FIGURE 2-9
CONCENTRATION FLOW -20 LBS/SEC
RELEASE RATE

3.0 PROBABILISTIC ASSESSMENT

3.1 Introduction

An analysis was performed to estimate the frequency with which a flammable concentration of natural gas would occur at selected building intakes at the Midland site from a hypothetical natural gas pipeline accidents.

This probabilistic assessment considered the frequency of pipe rupture, Gaussian dispersion of the gas plume and plume buoyancy. Meteorological parameters were selected to provide a realistic description of the events.

Results of the analyses are presented in Table 3-1. The predicted frequency of occurrence of a flammable concentration of gas at a safety-related air intake is less than 10^{-7} per year. For example, the frequency at the Control Room, Auxiliary and Diesel Generator building air intakes is 6.5×10^{-8} per year. However, for certain non-safety-related buildings close to the pipeline, i.e., the Evaporator building, the Combination Shop, the Mechanic Shop, and the Condensate Return Pumphouse, the frequencies are approximately 10^{-5} per year.

3.2 Method of Analysis

The predicted frequency of occurrence of a flammable concentration of gas at an intake at the plant is

$$P=P_R \sum_k^K l_k \left[\sum_n^N \sum_m^M \sum_j^J \left(P_I(k,n,m,j) \times P_W(n,m,j) \times \text{MRISE}(k,n,m,j) \right) \right]$$

- where:
- P = Frequency of occurrence of a flammable mixture of gas at an intake
 - P_R = Frequency of pipe rupture per unit length ($\text{yr}^{-1}\text{ft}^{-1}$)
 - P_I = Probability of gas plume with greater than the lower flammable limit concentration intercepting the intake given the stability class n , the wind speed m and direction j , and the distance between the midpoint of the segment k and the intake.
 - P_W = Probability that wind direction is j , the stability category is n and the wind speed is m .
- MRISE = Factor to account for plume buoyancy. MRISE is equal to zero if plume clears all structures on the way to the intake and then clears the intake itself. Otherwise, MRISE is equal to one. MRISE is dependent on the stability class, the wind speed and direction, and the distance between the segment and any building in the plume's path.
- l_k = Length of pipe segment k (ft)
 - K = Total number of segments into which the pipe is divided
 - N = Number of stability classes considered
 - M = Number of wind speeds considered
 - J = Number of wind directions considered

As can be seen from the above equation, the pipeline is divided into segments, and the total frequency is the sum of all the frequencies from each individual segment for all possible meteorological conditions. The number of segments was chosen based on calculations which were repeated with an increasing number of segments to show that the results converged.

The parameters in the above equation are discussed in detail in the following subsections.

3.2.1 Frequency of Pipe Rupture

The frequency of pipe rupture per unit length is determined from data collected by the American Gas Association (3.1). These data show that over a six year period (1970 to 1975 inclusive), there were 2,208 reportable service incidents for 275,000 miles of steel pipe. In addition, Reference 3.1 states that approximately 33 percent of all reportable incidents were classified as ruptures. Thus, the frequency of pipe rupture per unit length was calculated as follows:

$$\begin{aligned} \text{Pipe rupture frequency} &= \frac{2208 \text{ incidents}}{275,000 \text{ miles}} \times \frac{1}{6 \text{ yr}} \times \frac{1}{5280 \text{ft/mi}} \times \frac{.33 \text{ rupture}}{\text{incident}} \\ &= 8.36 \times 10^{-8} \text{ ruptures/ft-yr} \end{aligned}$$

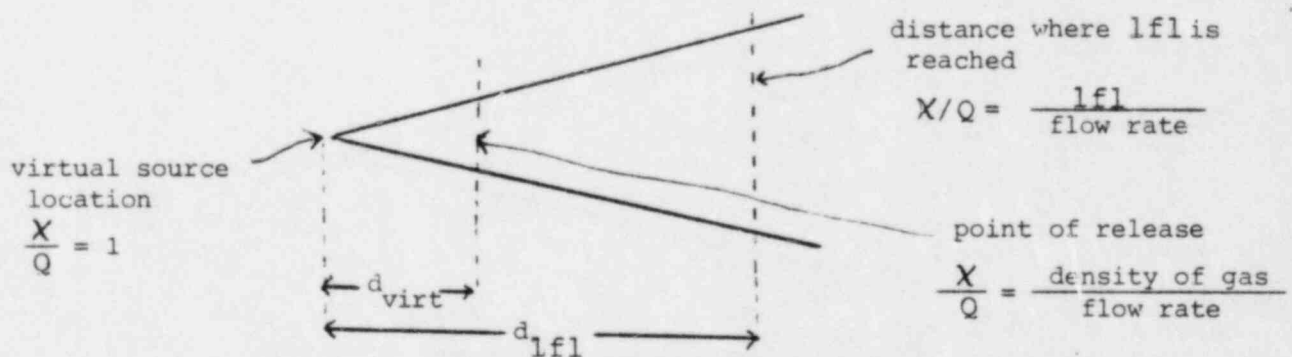
The pipe rupture frequency derived above is applicable to the portion of the pipeline which runs around the perimeter of the plant. For the onsite (inlet) portion of the pipeline, administrative and/or physical controls will be used to preclude pipe ruptures due to outside force. The data collected for the American Gas Association for 1974 and 1975 shows that 498 of the 824 reportable incidents were due to outside force. Thus, the pipe rupture frequency per unit length from other than outside forces for the onsite portion is given by

$$\begin{aligned} \text{Pipe rupture frequency} &= 8.36 \times 10^{-8} \frac{\text{ruptures}}{\text{ft-yr}} \times \frac{824-498}{824} \\ &= 3.31 \times 10^{-8} \frac{\text{ruptures}}{\text{ft-yr}} \end{aligned}$$

3.2.2 Determination of Pipe Length of Interest

A pipe segment will contribute to a flammable gas hazard at an intake only if the centerline concentration of a gas plume from this segment is above the lower flammable limit when it arrives at the intake. Therefore, if the intake is far enough away from the pipe segment, the centerline concentration of a plume would fall below the lower flammable limit before it reaches the intake, and this pipe segment would not contribute to the risk.

The dilution of the plume is calculated using conventional Gaussian dispersion. The maximum downwind distance the plume travels before its centerline concentration falls below the lower flammable limit (lfl) is determined by calculating the dispersion factor (X/Q) which corresponds to the lfl at the plume center and then determining the downwind distance to achieve that X/Q . The requisite X/Q at the lfl is the lfl divided by the flow rate. The downwind distance to achieve this limiting X/Q is denoted as d_{lfl} . This distance is then adjusted to account for the initial finite size of the plume by placing a virtual source at a distance of d_{virt} upwind from the point of release. The distance d_{virt} is chosen such that at this distance, the X/Q is equal to the density of the gas divided by the flow rate. (See diagram below)



Therefore, for a pipe segment to contribute to a risk at an intake, the maximum distance between this pipe segment and the intake is DLFL where

$$DLFL = d_{lfl} - d_{virt}$$

The total length of pipeline that could contribute to the flammable gas risk at an intake is that section of the pipeline that lies in a circle O_I of radius R_I , (See Figure 3-1).

where $R_I = DLFL + R_{II}$

$$R_{II} = \text{radius of circle } O_{II}$$

O_{II} = circle which encompasses
the entire building where
the intake is located

This total length of pipeline is then divided into smaller segments in order to calculate frequencies.

3.2.3 Probability of Wind Direction, Stability Category and Wind Speed, $P_W(n,m,j)$

The probability of a flammable gas hazard at an intake from a pipe segment is directly related to the probability that a wind will blow from that segment towards the intake. For this analysis, the probability of wind direction as a function of wind speed and stability class is obtained from a study of the Midland onsite meteorological data for the five year period March 1, 1975 through February 29, 1980 (3.2)

3.2.4 Probability of Plume Interception, $P_I(k,n,m,j)$

The probability of plume interception is dependent on the plume width, the radius of the intake circle, and the distance between the pipe segment and the center of the intake circle. Specifically, if a gas plume is to contribute to the hazard at an intake, a part of the flammable portion of this plume would have to be within the intake circle. Therefore, from any point on the pipeline, the maximum total angle a plume can be located within and still intercept the intake circle is the angle subtended by the intake circle plus the angle subtended by the total width of the flammable portion of the plume, (See Figure 3-2).

The intake circle is defined as a circle that covers the entire building where the intake is located. The half width of the flammable portion of the plume is the distance from the plume centerline to the lfl in the horizontal crosswind direction. This distance is calculated using the following formula derived from Slade. (3.3)

$$y = \sigma_y \left[2 \ln \left(\frac{Q}{\pi \sigma_y \sigma_z \bar{u} \text{lfl} \rho} \right) \right]^{\frac{1}{2}}$$

- where:
- y = distance from centerline of plume to lfl in the horizontal crosswind direction (m)
 - Q = pipe break flow rate (g/sec)
 - σ_y, σ_z = standard deviation of the gas concentration in the horizontal crosswind and vertical crosswind direction respectively (m)
 - \bar{u} = wind velocity (m/sec)
 - lfl = lower flammable limit in volume percent
 - ρ = density of gas (g/m^3)

As mentioned previously, the probability of plume interception is calculated based on the angles subtended by the intake circle and the plume width centered on the line connecting the pipe segment midpoint and the center of the intake circle. These angles (θ and ϕ in Figure 3-2) are calculated using simple geometry. The orientation (direction with respect to due north) of the line connecting the segment midpoint to the center of the circle is calculated based on the location of the pipe segment with respect to the location of the intake. Since the angles between each directional sector (N, NNE, NE, etc.) and due north are also known, the fraction of all directional sectors covered by the flammable portion of a plume can readily be calculated. If a directional sector (j) lies completely within the angle $\theta + 2\phi$ given on Fig. 3-2, $P_I(k,n,m,j) = 1$. If it lies completely outside, $P_I(k,n,m,j) = 0$. If an angle $\eta < 22.5^\circ$ overlaps $\theta + 2\phi$, $P_I(k,n,m,j) = \eta/22.5$.

For all directional sectors covered by the plume, the fraction of directional sector covered is multiplied by the probability of wind $P_W(n,m,j)$ from that direction to yield a wind-rose weighted by the plume interception probability.

3.2.5 Probability of Plume Clearance

As mentioned before, the section of pipe that could contribute to the risk is limited to the distance at which the centerline concentration would fall below the lfl. Another limitation is that a section of pipe will contribute to the risk only if the plume from this section will not clear the height of the intake.

For the purpose of this analysis, it was assumed that the natural gas would rise because it is less dense than air. This has been confirmed by emergency shut-down system tests conducted by the Consumers Power Company Gas Department

personnel. Personnel performing these tests have observed the gas to rise when released. (During the tests, natural gas is intentionally released at pressures which closely resemble conditions from a pipeline break.)^{3.8} The height of the plume rise is dependent on the downwind distance, the stability class and wind speed. For this analysis, the height of the plume centerline is estimated using the formulas of Briggs (3.4) Cloud centerline concentration is based on a Gaussian plume with initial finite size accounted for by a virtual source location.

From Briggs,

$$F = \frac{gV}{\pi} \left(1 - \frac{\rho_{NG}}{\rho_A}\right)$$

$$s = \frac{g}{T} \frac{\delta\theta}{\delta z} = \frac{g}{T} \left(\frac{\delta T}{\delta z} + 0.0098 \frac{^\circ K}{m}\right)$$

$$X^* = 2.4 u s^{-1/2}$$

$$h = 1.6 F^{1/3} u^{-1} x^{2/3} \text{ for } x < X^*$$

$$h_{\max} = 2.9 \left(\frac{F}{u s}\right)^{1/3} \text{ for } x \geq X^*$$

where:

h = plume rise (m)

F = buoyancy flux parameter (m^4/sec^3)

u = wind speed (m/s)

x = horizontal distance downwind (m)

V = volume flux of gas (m^3/sec)

s = stability parameter (sec^{-2})

$\frac{\delta T}{\delta z}$ = vertical temperature gradient of atmosphere ($^\circ K/m$)

θ = average potential temperature of air = $T + 0.0098 z$

g = gravitational acceleration = $9.78 m/sec^2$

ρ_A = density of air (g/m^3)

T = atmospheric temperature ($^\circ K$)

ρ_{NG} = density of natural gas (g/m^3)

X^* = capping distance (m)

z = vertical distance (m)

The temperature change with height ($^{\circ}\text{C}/100\text{m}$) is obtained from Table 1 of USNRC Regulatory Guide 1.23 and is listed below:

<u>Stability Classification</u>	<u>Pasquill Categories</u>	<u>Temperature Change with Height ($^{\circ}\text{C}/100\text{m}$)</u>
Extremely unstable	A	$\Delta T/\Delta z \leq -1.9$
Moderately unstable	B	$-1.9 < \Delta T/\Delta z \leq -1.7$
Slightly unstable	C	$-1.7 < \Delta T/\Delta z \leq -1.5$
Neutral	D	$-1.5 < \Delta T/\Delta z \leq -0.5$
Slightly stable	E	$-0.5 < \Delta T/\Delta z \leq 1.5$
Moderately stable	F	$1.5 < \Delta T/\Delta z \leq 4.0$
Extremely stable	G	$4.0 < \Delta T/\Delta z$

The above equations for plume rise hold for the more stable weather conditions (Classes E, F & G). For this analysis, it is assumed that the distance for plume clearance for Classes C & D are the same as the distance for Class E. This is conservative because at a fixed distance, plume height is greater for Classes C & D than it is for Class E. Stability Classes A and B were not included in this calculation. This is based on preliminary calculations which show that Classes A and B do not contribute to the risk because a plume would be rapidly diluted in these conditions.

For this analysis, it is conservatively assumed that a plume will clear a building only if the lfl edge of this plume in the vertical crosswind direction clears the building. The distance from the plume centerline to this lfl edge is calculated using the following equation derived from Reference 3.3.

$$z_0 = \sigma_z \left(2 \ln \frac{X_{cl}}{X_z} \right)^{1/2}$$

where

z_0 = half width of flammable plume in the vertical crosswind direction (m)

σ_z = standard deviation of the gas concentration in the vertical crosswind direction (m)

X_z = concentration at lfl edge and is equal to the product of the lfl and the density of the gas (g/m^3)

X_{cl} = cloud centerline concentration and is determined from a virtual source located at a distance d_0 upwind of the actual source. d_0 is chosen such that $X_{cl}=1$ at $d=d_0$ (g/m^3)

Plume clearance is then calculated. (See Figure 3-3)

$$\text{Clearance} = \Delta h - H - z_0$$

where Δh = height of plume centerline (m)

z_0 = half width of flammable plume in vertical crosswind direction (m)

H = height of building (m)

Before a bouyant plume can be assumed to clear an intake, this plume not only has to clear the height of the building where the intake is located, it also has to clear all structures in its path, i.e., if there are obstacles between the pipe

rupture and the building intake, these obstacles might destroy the plume buoyancy before it reaches the intake. For this calculation, it is assumed that if a plume fails to clear any structure on its way to the intake, plume buoyancy is destroyed and credit is not take for plume rise.

3.3 Input Parameters Used

The effective heights and radii of buildings which could intercept the plume are tabulated in Table 3-2. The effective building heights are calculated as shown:

$$\text{Effective Height} = \Delta H + (1.5xH)$$

Here, ΔH is the difference between the pipeline elevation and the plant grade. Since pipeline elevation is 600' and the plant grade is at El. 634'-0", ΔH is equal to 34 ft. H is the height of the building where the intake is located. The factor of 1.5 is an empirical factor used to account for wake effects. This factor is used for all buildings on the site with the exception of the Reactor Containment buildings. Studies (3.7) show that the cavities formed behind an aerodynamically smooth structure, for example a sphere, do not exceed the height of that structure by any appreciable amount. Because of their hemispherical tops, the effective height of the Reactor Containment buildings can thus be approximated by the height of these buildings with no correction for wake effects.

The section of gas pipeline that will be used to transport natural gas to the Midland site is shown in Figure 3-4. (3.5,3.6) For this analysis, this pipeline is divided into

two sections - the perimeter section and the inlet section. Figure 3-4 shows the location of these sections and the buildings (areas) of concern. Evaluations were performed for both the perimeter and the inlet sections of the pipeline. For perspective, Figure 3-5 shows approximate distances between the pipeline and two buildings of concern.

The gas will mix rapidly with the air as it emerges from the break because it will be a high momentum jet. For this situation, Marshall^{3.9} argues that the gas will mix rapidly with the ambient air and the kinetic energy initially contained in the jet will be converted to heat; hence, even though the jet will at first be cooled as it emerges from the broken pipe, the rapid mixing will ensure that it does not remain cool for a significant time. Therefore, it was assumed in this analysis that the plume emerges at ambient temperature. In these conditions, the density of natural gas relative to that of air is 0.61 and the lfl is 5 percent by volume.

In order to investigate the sensitivity of the results to assumptions about the plume density, the effect of assuming that the gas could be cooled down by one or two degrees per atmosphere change in pressure due to the expansion process was also investigated. Results of this sensitivity study are reported in Appendix A.

The flow rate of natural gas in the pipeline used in this analysis is 20 lbs/sec. This flow rate is approximately 35 percent higher than the maximum demand required for the boilers.

3.4 Results of the Probabilistic Calculations

A summary of the calculated results by intake location is presented in Table 3-1.

The summed frequency for all wind speeds, weather conditions and pipe break locations of a flammable concentration of gas reaching the majority of the intakes is less than 10^{-7} per year. The exception to this is for some non-safety-related buildings that are close to the pipeline. For these buildings (the Evaporator building, Combination Shop, Mechanic Shop, and the Condensate Return Pumphouse), the frequency is approximately 10^{-5} per year.

Results from Table 3-1 are for a break flow rate of 20 lbs/sec. A reduction in this break flow rate would reduce the gas concentration within the plume. However, this reduction in flow rate will also reduce the buoyancy of the plume due to the reduction of the buoyancy flux parameter, (See Section 3.2.5). Hence, a reduction in flow rate would not necessarily lead to a reduction in predicted frequencies because the plume might fail to rise above buildings that would be cleared for a higher flow rate. Therefore, a sensitivity study was performed to determine the relationship between the frequency of flammable gas at an intake and the reduction in break flow rate. Results of this study, which was performed using the Control Room, Auxiliary and Diesel Generator building intakes and the Evaporator building intakes with the perimeter section of the pipeline as the source, are presented in Table 3-3. From this table, it can be seen that the risk of a flammable hazard at the intake decreases as the break flow rate decreases. Therefore, for a maximum break flow rate of 20 lbs/sec, the maximum probabilities are those shown in Table 3-1.

Although the results of this analysis are based on realistic input, they are still believed to be a conservative estimate of the true frequency of a flammable concentration of gas at the intake. Specific items of conservatism are as follows:

- o The intakes are assumed to be always open.

- o When calculating the effective height of the building, the building height was increased by a factor of 1.5 to account for wake effects of this building. (The Reactor Containment building is the only exception to this).
- o When calculating the plume clearance, the entire plume was assumed to be non-buoyant if any portion of the plume with greater than the lfl failed to clear a building.
- o The area of the circles drawn around the buildings is larger than the areas of concern.

3.5 Conclusion

A probabilistic analysis has been carried out to show that the predicted frequency with which flammable concentrations would occur at the intakes of all safety-related structures, given a break in the gas pipeline, does not exceed 10^{-7} per year.

Other buildings near the safety-related structures were also evaluated. It was determined that some of these non-safety-related buildings will not exceed the 10^{-7} per year frequency criteria. For those buildings which exceed 10^{-7} per year frequency, further work is underway in order to confirm that these buildings pose no threat to safety-related structures even if they fill with gas and explode.

3.6 References for Section 3

- 3.1 J. F. Kiefner and R. B. Smith, "An Analysis of Reportable Incidents for Natural Gas Transmission and Gathering

Lines, 1970 through 1975," to Pipeline Research Committee, American Gas Association, NG-18 Report No. 106, (August 5, 1977).

- 3.2 Internal Correspondence between H. Firstenberg, R. B. Jubach and K. Toth. REC-81-94 (EC) dated 6-11-81.
- 3.3 D. H. Slade, "Meteorology and Atomic Energy 1968," U. S. Atomic Energy Commission, July 1968.
- 3.4 G. A. Briggs, "Plume Rise," TID 25075, Nov. 1969.
- 3.5 Consumers Power Company Drawing, "Proposed H. P. Main Extension to Serve Midland Nuclear Plant in Midland County," TLM/GAS No. 1452273, Tax Code No. 565200, Revised 2-10-82.
- 3.6 Letter from Mike Ferens, CPCo, to K. Toth, NUS. Received 7-26-82.
- 3.7 F. Kreith, 'Principles of Heat Transfer', Section 9.1, 1958.
- 3.8 Letter from J. D. Gribble, M-325, CPCo Gas Department to M. A. Ferens, P24-615, CPCo, September 21, 1982.
- 3.9 J. G. Marshall, "The Size of Flammable Clouds Arising from Continuous Releases Into the Atmosphere - Part 2 " in Chemical Process Hazards VII, Institute of Chemical Engineers Symposium Series No. 58 pp 11 et seq (1980).

TABLE 3-1
 RESULT SUMMARY - ANNUAL FREQUENCY OF FLAMMABLE GAS CONCENTRATION
 REACHING SPECIFIC BUILDING AIR INTAKES

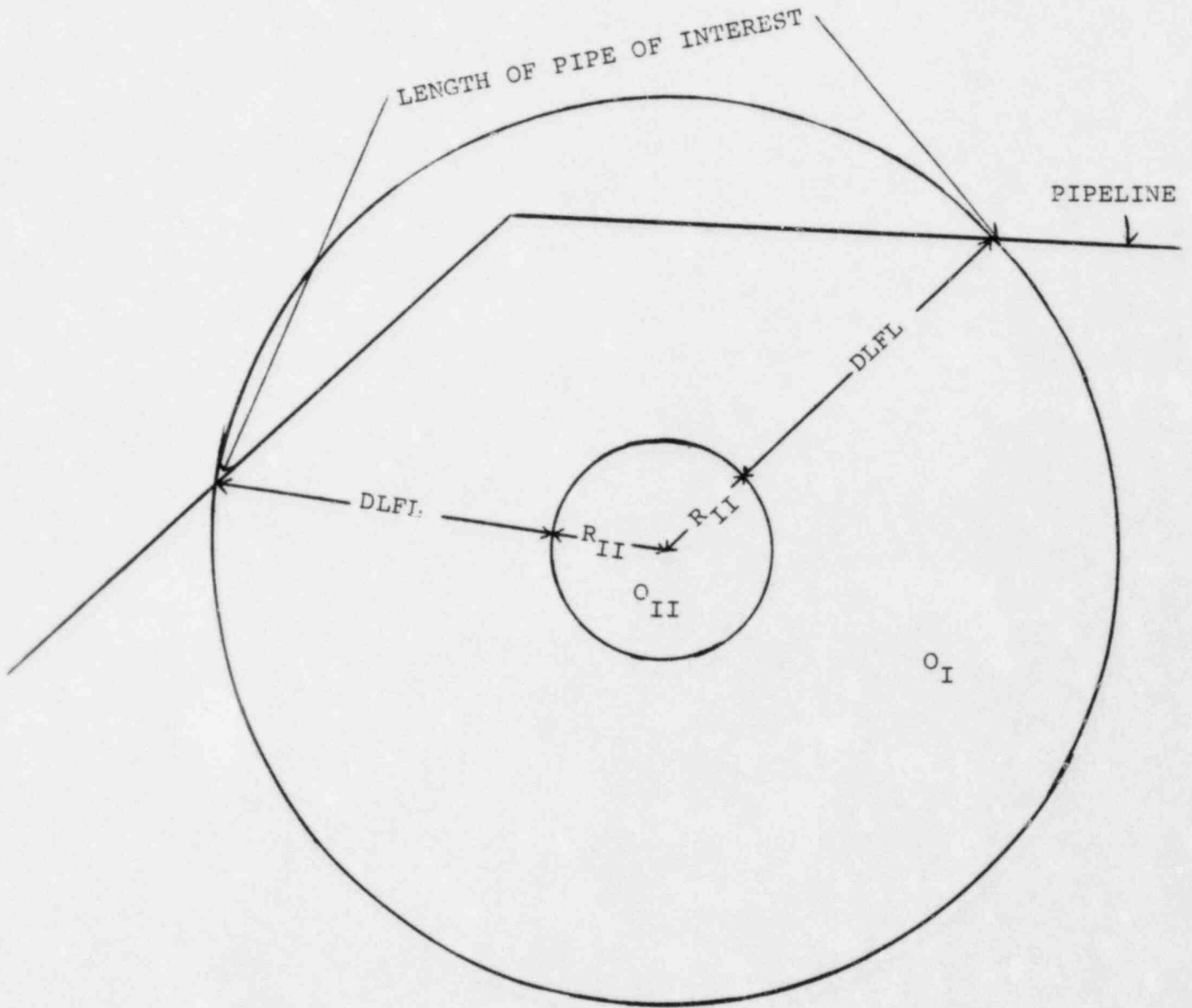
<u>Building</u>	<u>Frequency From Pipeline on Perimeter of Site</u>	<u>Frequency From Inlet Section of Pipeline</u>	<u>Total Frequency of Flammable Gas Concentration at Building Intake</u>
Service Water Pump Structure	1.4×10^{-9}	3.4×10^{-9}	4.8×10^{-9}
Control Room, Auxiliary and Diesel Generator Building Air Intakes	5.3×10^{-8}	1.2×10^{-8}	6.5×10^{-8}
Evaporator Building	3.8×10^{-6}	8.7×10^{-6}	1.3×10^{-5}
Combination Shop	3.7×10^{-7}	5.9×10^{-6}	6.3×10^{-6}
Warehouse	2.6×10^{-6}	9.5×10^{-8}	2.7×10^{-6}
Technical Support Center	4.3×10^{-8}	4.2×10^{-8}	8.5×10^{-8}
Mechanic Shop	1.6×10^{-5}	2.9×10^{-8}	1.6×10^{-5}
Condensate Return Pumphouse	9.7×10^{-6}	8.9×10^{-9}	9.7×10^{-6}
Office Building	6.2×10^{-8}	1.3×10^{-8}	7.5×10^{-8}
Change House	5.9×10^{-9}	4.2×10^{-9}	1.0×10^{-8}
Administration Building	3.9×10^{-9}	4.9×10^{-9}	8.8×10^{-9}

TABLE 3-2
BUILDING PARAMETERS

<u>Building</u>	<u>Radius</u> <u>(ft)</u>	<u>Effective</u> <u>Height</u> <u>(ft)</u>
Service Water Pump Structure	72	76
Diesel Generator & Control Room & Turbine Building	160	188
Evaporator Building	172	138
Combination Shop	130	94
Warehouse	222	87
Technical Support Center	56	79
Mechanic Shop	55	72
Condensate Return Pump House	27	72
Office Building	121	87
Change House	126	72
Administration Building	89	124
Reactor Building Unit #1	62	188
Reactor Building #2	62	188
Auxiliary Building	166	188
Circulating Water Intake Structure	89	73
Solid Radwaste Building	101	94

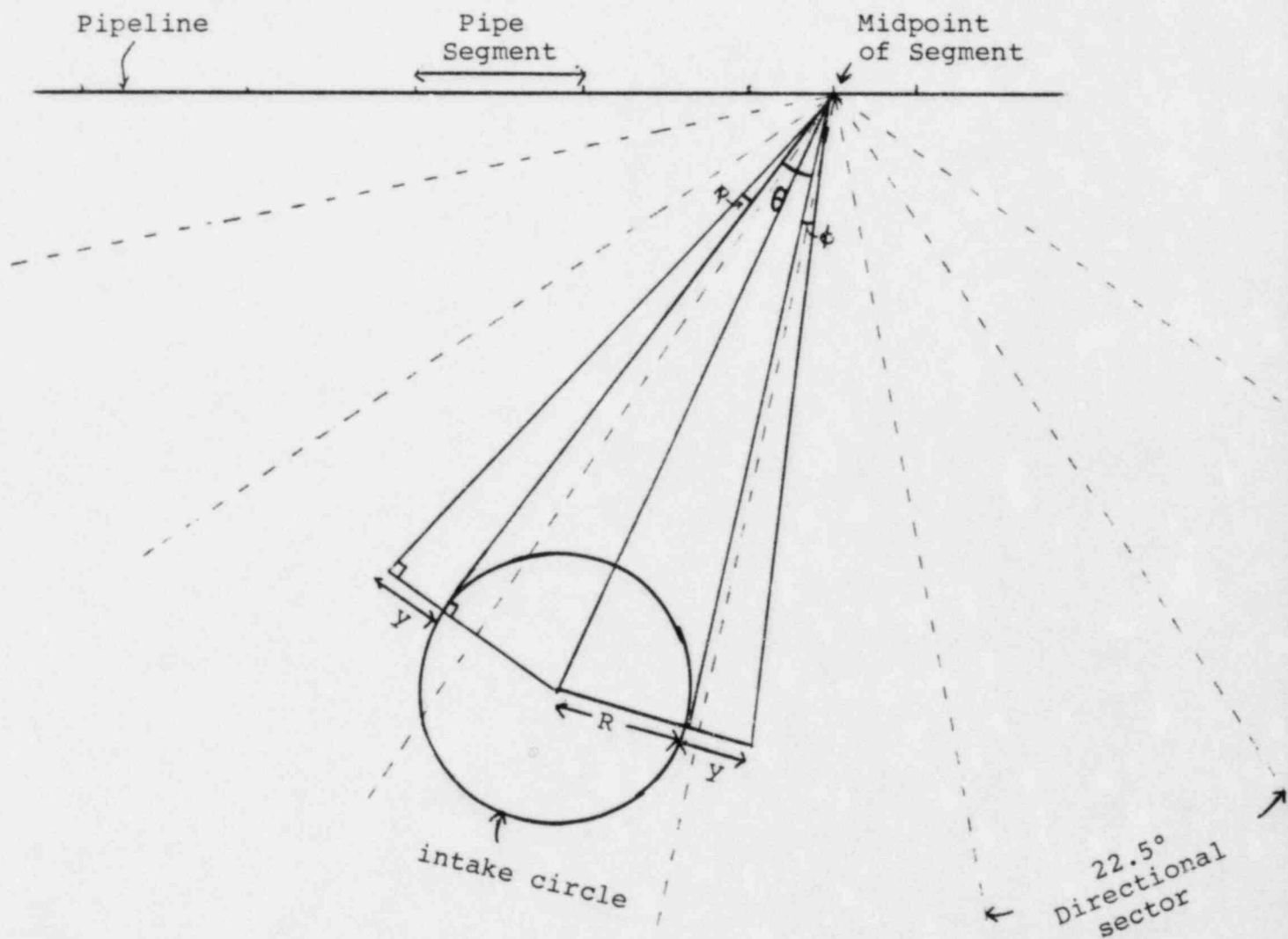
TABLE 3-3
 SENSITIVITY OF FREQUENCY TO BREAK FLOW RATE

<u>Break Flow Rate (lb/s)</u>	<u>Control Room Diesel Generator Intakes</u>	<u>Evaporator Building Intakes</u>
20	5.3×10^{-8}	3.8×10^{-6}
15	3.6×10^{-8}	3.1×10^{-6}
10	1.3×10^{-8}	2.1×10^{-6}
5	1.1×10^{-9}	8.4×10^{-7}



- O_I = circle where a flammable concentration of gas may affect intake
- O_{II} = intake circle
- R_{II} = radius of intake circle
- DLFL = distance to achieve the lower flammable limit less the virtual source distance

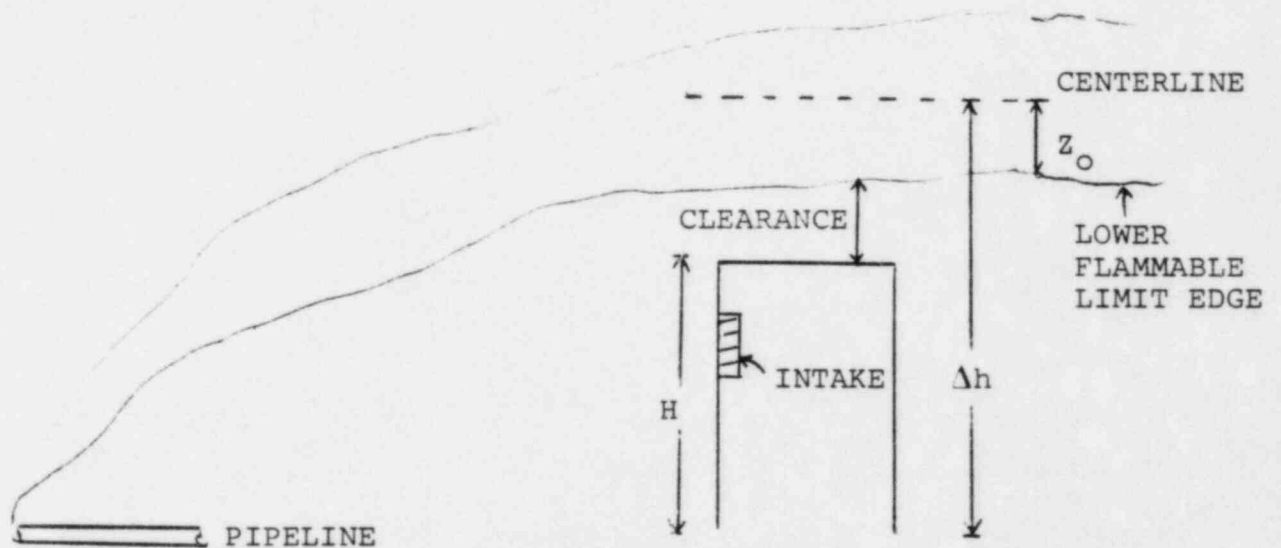
FIGURE 3-1
DETERMINATION OF PIPE LENGTH OF INTEREST



R = radius of intake circle
 y = half width of plume
 r = distance from plume centerline to lfl edge
 θ = angle subtended by intake circle
 ϕ = angle subtended by y

FIGURE 3-2

DETERMINATION OF PROBABILITY OF INTERCEPTION



z_0 = half width of flammable plume in the vertical crosswind direction

Δh = height of plume centerline

H = height of building

$$\text{Clearance} = \Delta H - H - z_0$$

FIGURE 3-3
PLUME CLEARANCE

INLET SECTION OF

PERIMETER SECTION OF PIPELINE

MECHANICAL SHOP

CONDENSATE RETURN PUMPHOUSE

WATER HOUSE

PROJECT FIELD OFFICE

CHANGE HOUSE

TIME OFFICE

WATER STORAGE TANK

WELDERS TOOL SHED

GUARD HOUSE

EXHAUSTION TOWER
EXHAUSTION AND SUPPLY SILENCE BUILDING

TECH SUPPORT CNTR

AUXILIARY BUILDING

REACTOR BLDG UNIT

REACTOR BLDG UNIT

CONTROL ROOM

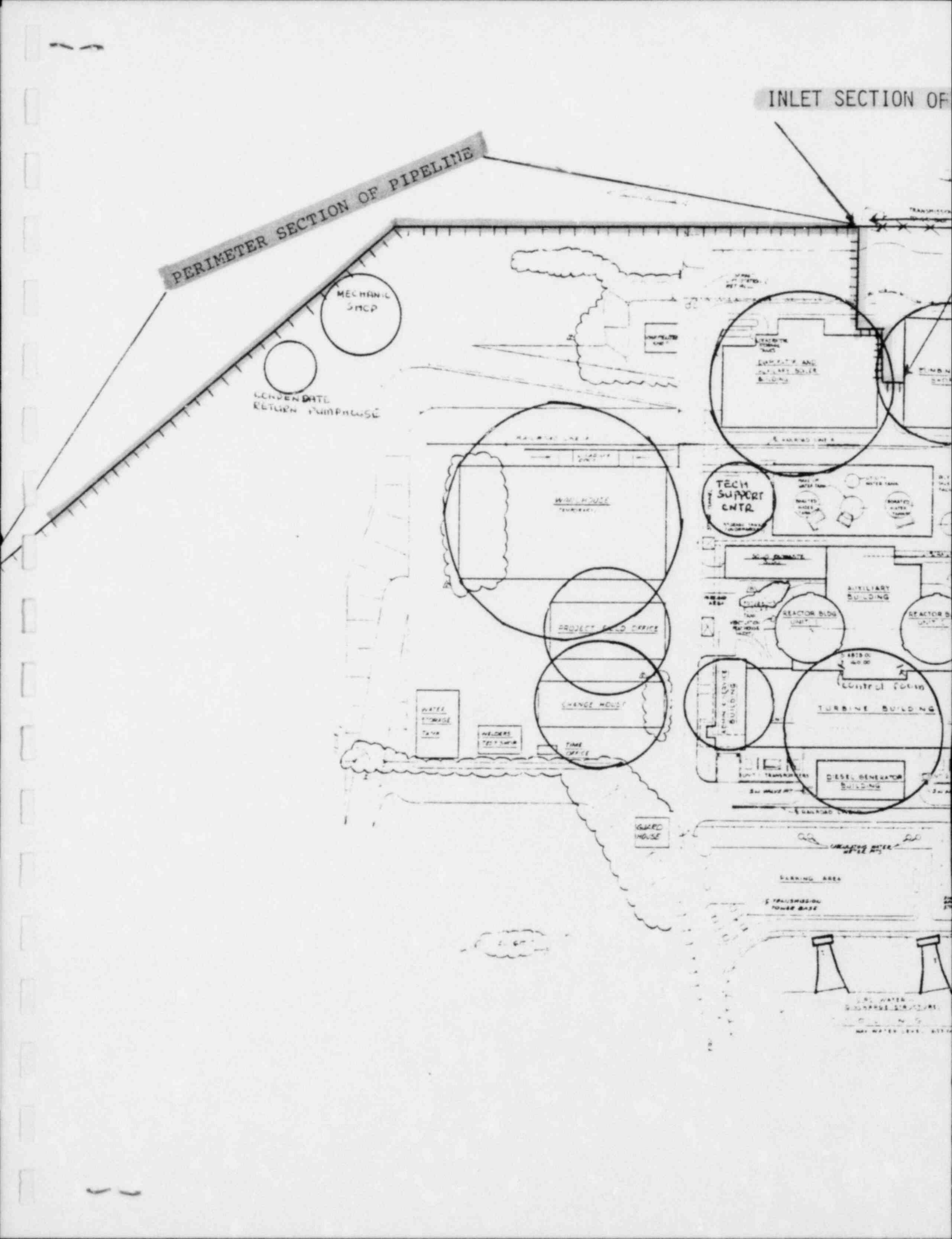
TURBINE BUILDING

DIESEL GENERATOR BUILDING

BURNING AREA

TRAILER/STORAGE TOWER BASE

LOW WATER DISCHARGE STRUCTURE
HIGH WATER LEVEL



INLET SECTION OF

PERIMETER SECTION OF PIPELINE

1605'

765'

MECHANICAL SHOP

CONDENSATE RETURN PUMPHOUSE

1132'

600'

TECH SUPPORT CNTR

PROJECT CONTROL ROOM

LABORATORY

WATER STORAGE TANK

INTEGRATED TELEPHONE

TRAIL

REACTOR BLDG

REACTOR

CONTROL ROOM
TURBINE BUILDING
DIESEL GENERATOR BUILDING

GUARD HOUSE

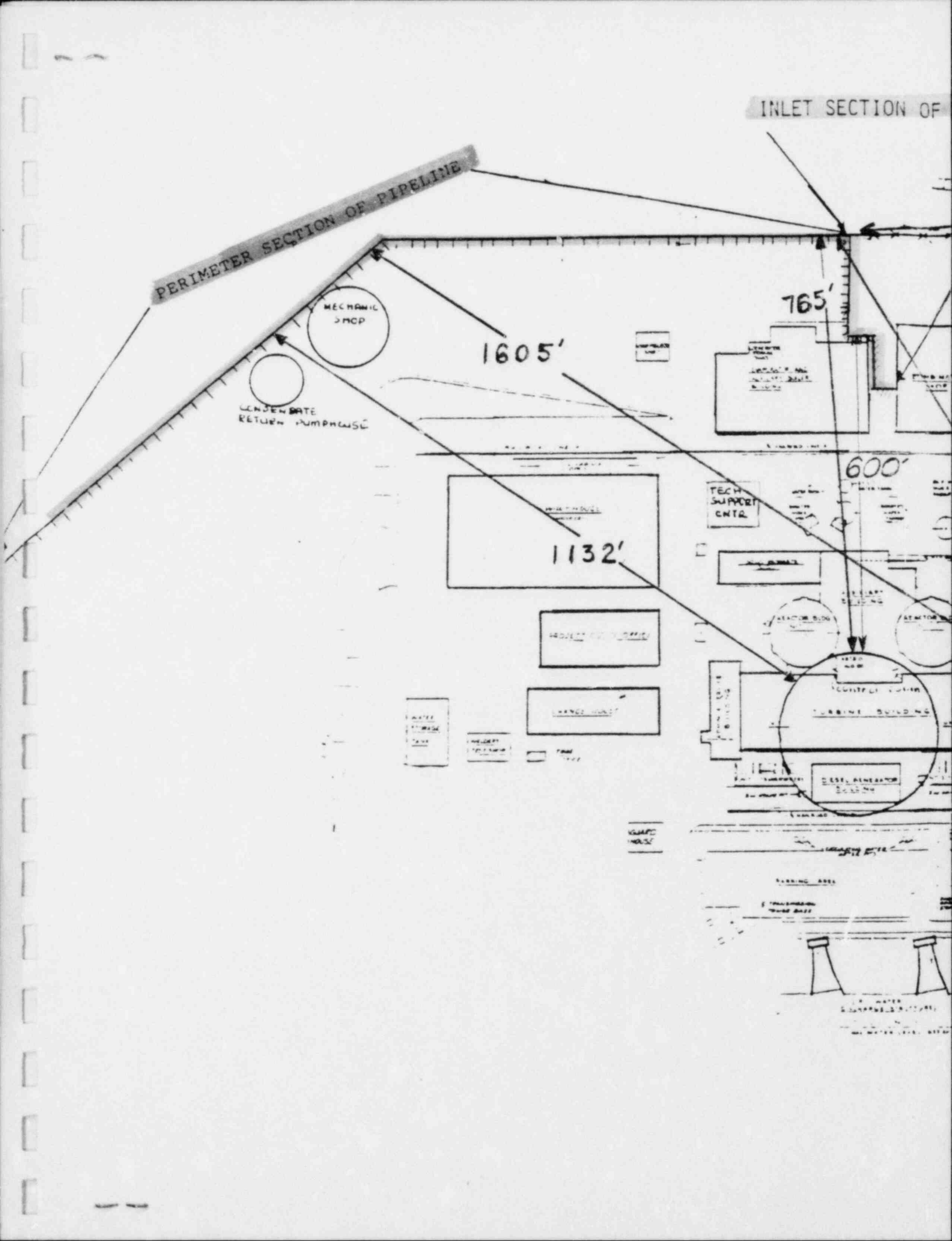
PARKING AREA

1 MILLION GALLON WATER TANK



1 MILLION GALLON WATER TANK

1 MILLION GALLON WATER TANK



PIPELINE

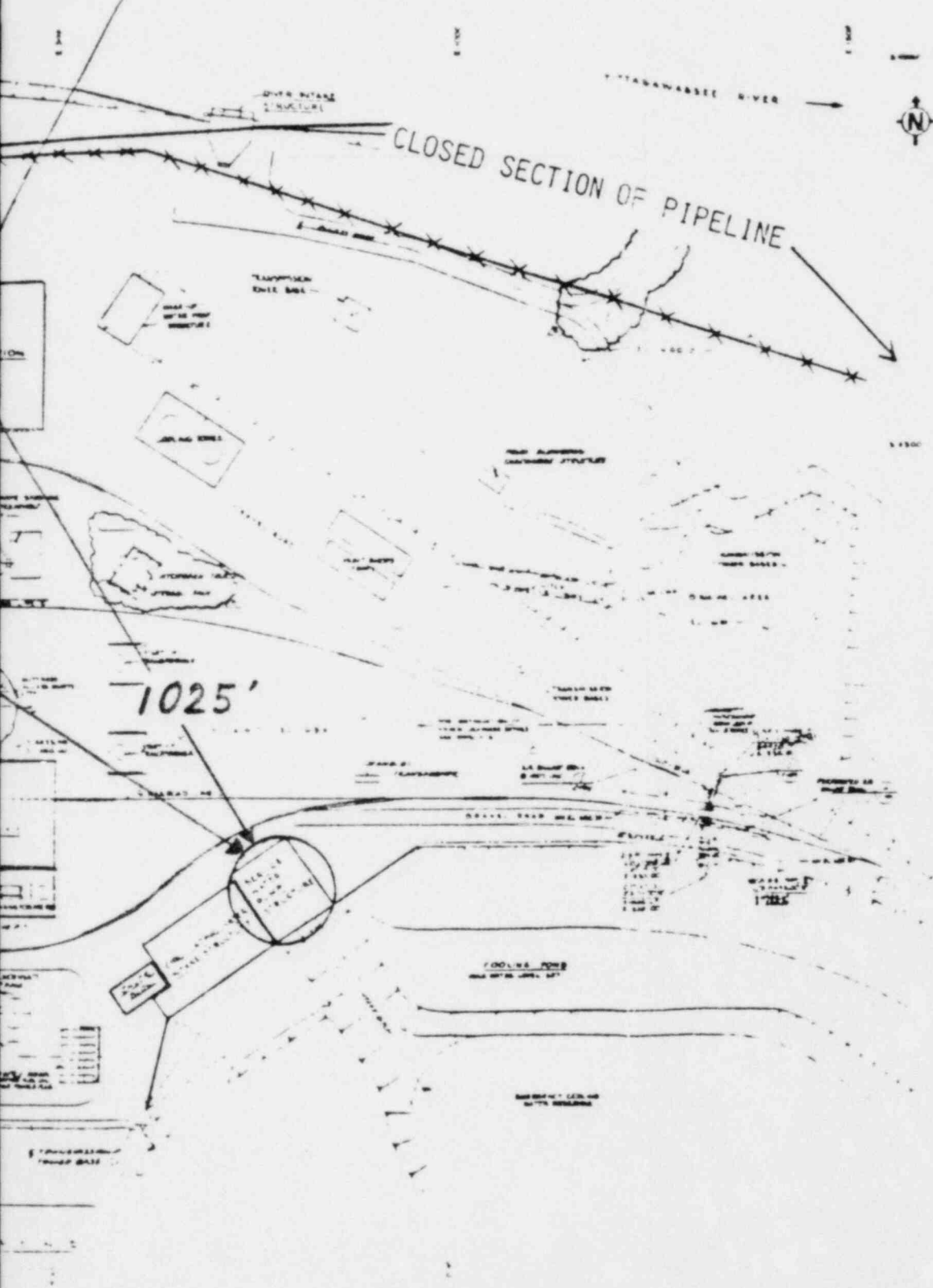


FIGURE 3-5

PIPELINE AND DISTANCE PERSPECTIVE

APPENDIX A
SENSITIVITY OF RESULTS TO GAS EXIT TEMPERATURE

This sensitivity study was performed to address a concern about the cooling of natural gas while escaping from a postulated break in a pressurized pipeline and expanding to atmospheric conditions.

An analysis was performed to determine the mass flow rate and temperature of the gas resulting from a postulated rupture in the natural gas pipeline. Using the COMPARE-MOD1 computer program, which models the gas flow as a polytropic flow process, it was determined that just prior to exit at the break, the temperature of the gas is between +3 to +28^o Fahrenheit. This gas temperature range was used in this sensitivity study. The gas is not expected to cool further upon leaving the pipe because of the dissipative jet effects and entrainment of the ambient air. (The Nuclear Regulatory Commission has a rule-of-thumb that states that there is a one to two degree Fahrenheit cooling per atmosphere change in pressure. Based on this rule-of-thumb and on the fact that the pipeline pressure is 400 psi, the gas is calculated to cool by approximately 30 to 60 ^oF. Therefore, if the temperature under normal flow conditions is 60^oF, the gas exit temperature would be between 30^oF and 0^oF. This agrees with the above mentioned COMPARE-MOD1 analysis).

Studies by the Consumers Power Company show that the specific gravity of natural gas is 0.61 at 60^oF. Assuming that the ideal gas law applies, the specific gravity of natural gas is then 0.65 and 0.7 for gas temperatures of 30^oF and 0^oF, respectively.

Using relative densities of 0.65 and 0.7, the frequency of flammable gas hazards at Midland site intakes were evaluated. Note that these densities of a cooler plume are used only for plume rise calculations. The relative density of gas at ambient temperature was used for all Gaussian dispersion calculations. The results of this evaluation are presented in Table A-1. The frequencies in this table are for the off-site (perimeter) section of the pipeline. The frequencies from the on-site section of the pipeline are not affected by the above density assumptions because no credit for plume buoyancy was taken when calculating frequencies from this on-site section. The total frequency (i.e., the frequency from both the off-site and inlet (on-site) pipeline) as a function of natural gas specific gravities at the rupture is presented in Table A-2. As can be seen from this table, the results do not change appreciably as a function of exit temperatures. Also, the conclusion that flammable concentrations do not occur at the intakes of safety-related structures with a frequency greater than 10^{-7} per year is unaffected.

TABLE A-1
 SPECIFIC GRAVITY EFFECT ON ANNUAL FREQUENCY OF
 FLAMMABLE GAS CONCENTRATION REACHING SPECIFIC BUILDING
 AIR INTAKES FROM PIPELINE ON PERIMETER OF SITE

	Specific Gravity <u>0.61*</u>	Specific Gravity <u>0.65</u>	Specific Gravity <u>0.7</u>
Service Water Pump	1.4×10^{-9}	1.4×10^{-9}	1.4×10^{-9}
Control Room, Auxiliary and Diesel Generator Building Air Intakes	5.3×10^{-8}	6.8×10^{-8}	7.7×10^{-8}
Evaporator Building	3.8×10^{-6}	3.9×10^{-6}	3.9×10^{-6}
Combination Shop	3.7×10^{-7}	4.0×10^{-7}	4.4×10^{-7}
Warehouse	2.6×10^{-6}	2.7×10^{-6}	2.9×10^{-6}
Technical Support Center	4.3×10^{-8}	5.2×10^{-8}	6.0×10^{-8}
Mechanic Shop	1.6×10^{-5}	1.6×10^{-5}	1.6×10^{-5}
Condensate Return Pumphouse	9.7×10^{-6}	9.7×10^{-6}	9.8×10^{-6}
Office Building	6.2×10^{-8}	7.4×10^{-8}	8.1×10^{-8}
Change House	5.9×10^{-9}	5.9×10^{-9}	6.2×10^{-9}
Administration Building	3.9×10^{-9}	3.9×10^{-9}	3.9×10^{-9}

* Repeated from column one of Table 3-1 for comparison

TABLE A-2
 RESULT SUMMARY OF SPECIFIC GRAVITY EFFECTS ON
 ANNUAL FREQUENCY OF FLAMMABLE GAS CONCENTRATION
 REACHING SPECIFIC BUILDING AIR INTAKES

	Specific Gravity <u>0.61*</u>	Specific Gravity <u>0.65</u>	Specific Gravity <u>0.7</u>
Service Water Pump Structure	4.8×10^{-9}	4.8×10^{-9}	4.8×10^{-9}
Control Room, Auxiliary and Diesel Generator Building Air Intakes	6.5×10^{-8}	8.0×10^{-8}	8.9×10^{-8}
Evaporator Building	1.3×10^{-5}	1.3×10^{-5}	1.3×10^{-5}
Combination Shop	6.3×10^{-6}	6.3×10^{-6}	6.3×10^{-6}
Warehouse	2.7×10^{-6}	2.8×10^{-6}	3.0×10^{-6}
Technical Support Center	8.5×10^{-8}	9.4×10^{-8}	1.0×10^{-7}
Mechanic Shop	1.6×10^{-5}	1.6×10^{-5}	1.6×10^{-5}
Condensate Return Pumphouse	9.7×10^{-6}	9.7×10^{-6}	9.8×10^{-6}
Office Building	7.5×10^{-8}	8.7×10^{-8}	9.4×10^{-8}
Change House	1.0×10^{-8}	1.0×10^{-8}	1.0×10^{-8}
Administration Building	8.8×10^{-9}	8.8×10^{-9}	8.8×10^{-9}

* Repeated from column three of Table 3-1 for comparison

NUS Corporation

910 Clopper Road
Gaithersburg, Maryland 20878
301/258-6000
TWX: 710-828-0540
NUSWASH

Domestic Offices

Aiken
Chicago
Clearwater
Columbia
Denver
Houston
Menlo Park
Pittsburgh
Portland
Rockville
San Diego
Sherman Oaks

International Offices

Brazil
Germany
Japan
Saudi Arabia
Venezuela
Yugoslavia

ATTACHMENT